PARSEC'S ASTROMETRY – THE RISKY APPROACH

A.H. ANDREI -- Observatório Nacional - ON/MCTI, Brasil
Osservatorio Astronomico di Torino – OATo/INAF, Italy
Observatoire de Paris – SYRTE/OP, France
Observatório do Valongo – OV/UFRJ, Brasil

Parallaxes - and hence the fundamental establishment of stellar distances - rank among the oldest, keyest, and hardest of astronomical determinations. Arguably amongst the most essential too. The direct approach to obtain trigonometric parallaxes, using a constrained set of equations to derive positions, proper motions, and parallaxes, has been labelled as risky. Properly so, because the axis of the parallactic apparent ellipse is smaller than one arcsec even for the nearest stars, and just a fraction of its perimeter can be followed. Thus the classical approach is of linearizing the description by locking the solution to a set of precise positions of the Earth at the instants of observation, rather than to the dynamics of its orbit, and of adopting a close examination of the never too many points available. **In the PARSEC program the parallaxes of 143 brown dwarfs were aimed at. Five years of observation of the fields were taken with the WIFI camera at the ESO 2.2m telescope, in Chile. The goal is to provide a statistically significant number of trigonometric parallaxes to BD sub-classes from L0 to T7**. Taking advantage of the large, regularly spaced, quantity of observations, here we take the risky approach to fit an ellipse in ecliptical observed coordinates and derive the parallaxes. We also combine the solutions from different centroiding methods, widely proven in prior astrometric investigations. As each of those methods assess diverse properties of the PSFs, they are taken as independent measurements, and combined into a weighted least-square general solution. The results obtained compare well with the literature and with the classical approach.

This work belongs to all participants of PARSEC and IPERCOOL projects

BD at a glance

Brown dwarfs are very low-mass stars whose masses (M < 0.075 Msol) are insufficient to sustain the core hydrogen fusion reactions that balance radiative energy losses. Supported from further gravitational contraction by electron degeneracy pressure, evolved brown dwarfs continually cool and dim over time as they radiate away their initial contraction energy, ultimately achieving photospheric conditions that can be similar to those of giant planets.

The first examples of brown dwarfs were identified as recently as 1995. Today, there are hundreds known in nearly all Galactic environments, identified largely in wide-field, red and near-infrared imaging surveys such as 2MASS, DENIS, SDSS and UKIDSS. The known population of brown dwarfs encompasses the late-type M (T*eff* ≈2500–3500 K), L (T*eff* ≈1400–2500 K) and T spectral classes (T*eff* ≈600–1400 K), while efforts are currently underway to find even coller members of the putative Y dwarf class.

- Low-mass stars, cooler than M dwarfs, extremely old, link between stars and planets.
- Need observations to complement the photometric & high proper motion identification.

BD at a glance

Because brown dwarfs cool over time, their spectral properties are inherently time dependent. However, the primary observables of a brown dwarf - temperature, luminosity and spectral type - depend on both mass and age (and weakly on metallicity). This degeneracy complicates characterizations of individual sources and mixed populations.
For instance, the Malmquist bias comes from the intrinsic dispersion in the absolute magnitude-colour relationship and a limited sample absolute magnitude definition. A given colour (or spectral type) does not correspond to a unique luminosity, but rather to a distribution due to intrinsic scatter in metallicity and age (and non detected binaries that appear brighter for their colour).

- Complex mass-luminosity-metallicity-age relation.
- Spectral type change with age.
- Need observations to constrain/test theoretical models.

BD at a glance

Low-mass dwarfs compose some 70% of all stars and nearly half of the stellar mass of the Galaxy. And perhaps 80% of the Solar neighborhood, which preferentially consists of relatively old objects. Therefore, the majority of low-mass BDs near the Sun should be T-type ones (older than 1Gy) - whereas young M-type BDs can probably only be found in young open clusters and associations, off the local border.

BDs hold cosmological, as well as Milky Way's, key evolutionary information since their long lives make them primordial objects. For the dynamics of galaxies, including our own, they offer clues on the baryonic contents and on the evolution of the galactic mass. For field star formation, their space and age distribution contribute to answer the basic questions about the variation of the initial mass function or indeed if there is a low limit mass of the formation region below which the birth of normal stars is inhibited.

BD bridge the gap between formatiion of dwarf stars and giant planets; their photosphere ultimately decaying onto hot Jupiters-like atmospheres. Their relatively undisturbed convection zone and thin chromosphere enable to study these zones, that are quite complex in normal stars.

- Need observations to take advantage of such probes

BD science drivers

- **Very low-mass (nearly) stars**
- **Main stellar component of the galaxy**
- **Galactic chronometers**
- **Sub-stellar IMF and low-mass cutoff for star formation**
- **Sub-stellar and hot-Jupiters atmosphere models**

BD critical problems

- **Degeneracy in the age-temperature relation – from the mass-luminosity one**
- **Complex dependencies of spectral type on *Teff, log(g), [Fe/H]***

BD observational constraint

- **Derivation of BDs absolute luminosities through the measurement of trigonometric parallaxes is essential to disentangle their physical properties**

BD trigonometric parallaxes at work

- **Distances determined independently of any model**
- **Calibration of the photometric and spectroscopic parallaxes for the classes and sub-classes of sub-dwarfs.**
- **The absolute luminosity to a large number of objects to derive the LF**
- **With distances and derived quantities the 3D and evolution map of the Solar neighborhood is traced**
- **By knowing the distance, then either large velocities and/or low lunminosities point out to sub-dwarfs**
- **With known distance, an excess of luminosity indicates binarys**
- **Determining the distance, then a model radius translates into temperatrure**
- **Determining the distance – hence the luminosity – then the spectral features translate into surface gravity**
- **Determining the distance, and the proper motion, enables to decide on membership**
- **Rich, scientifically outreaching, Solar neighborhood laboratory for the methods of determination of distances**

PARSEC at a glance

- measures parallaxes of 120 L and 23 T dwarfs brighter than z=20 in the southern hemisphere
  (most of these objects will not be observed by GAIA)

- using WFI on the ESO 2.2m, in the z band (compromise between optimal QE in I band and target typical brightness (I-z~2)

- started in 2007 and ended on early 2011, 4-6 epochs/year (Brasil-Italia cooperation which evolved to the consortium IPERCOOL/BR-IT-UK-CN)

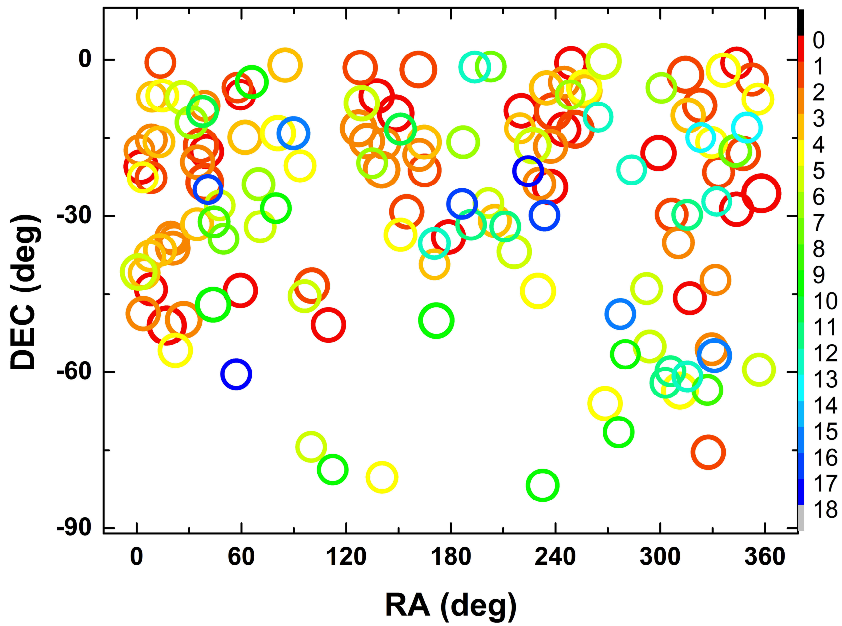

PARSEC Targets by sub-class

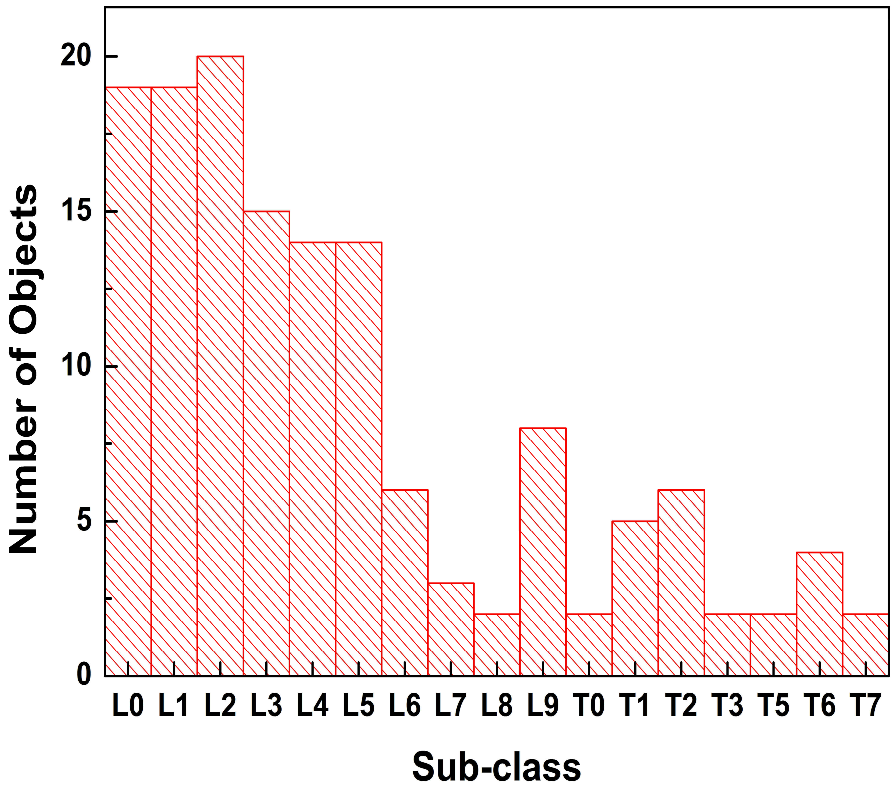

Catalogue data from www.dwarfarchives.org

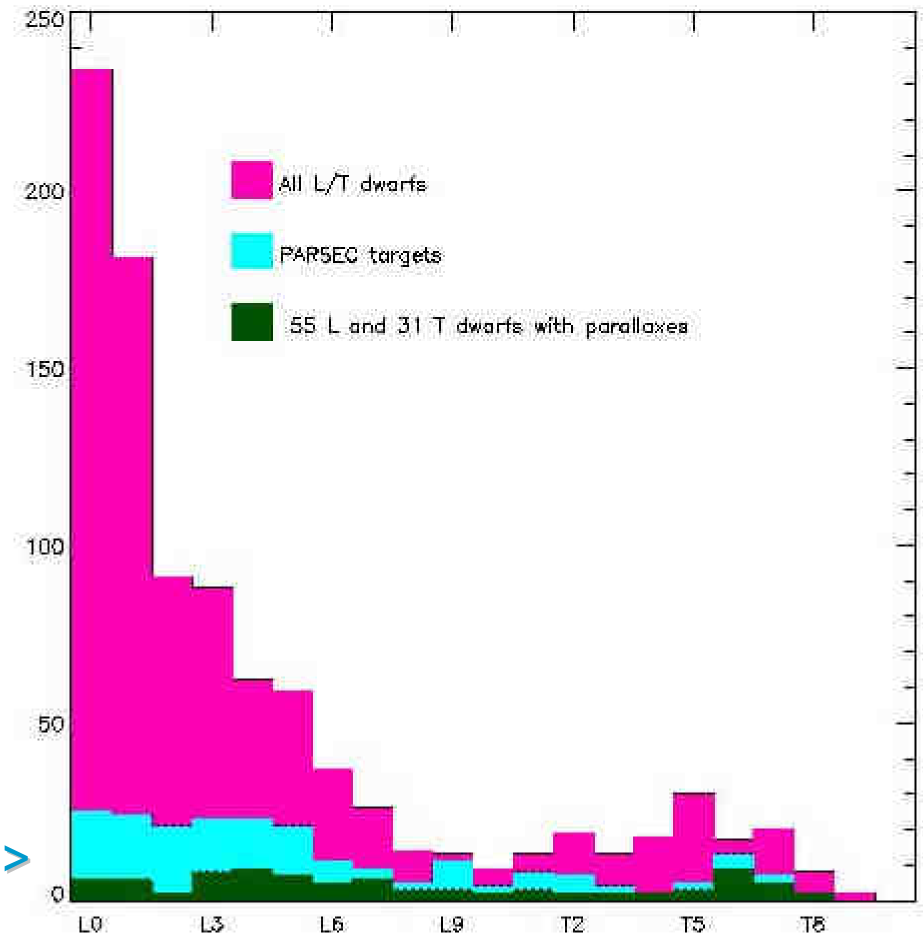

PARSEC Targets ->

Main Output

- **More than 100% increase of L dwarfs with trigonometric parallaxes**

- **Increment to at least 10 (in conjunction with published results) on the number of objects per spectral sub-class in the range L0 to T7**

- **Study the binarity fraction of brown dwarfs**

- **Single out interesting/benchmark objects for extended spectroscopic observation**

Additional Outputs

- **Proper motion catalogue of 197,500 2MASS stars on the 140 ~ 0.3 sq.deg fields using positions PARSEC for the second epoch**

- independent validation of UCAC2 proper motions
- search for fast-moving objects
- search for stellar companions
- brown dwarf candidate selection tool

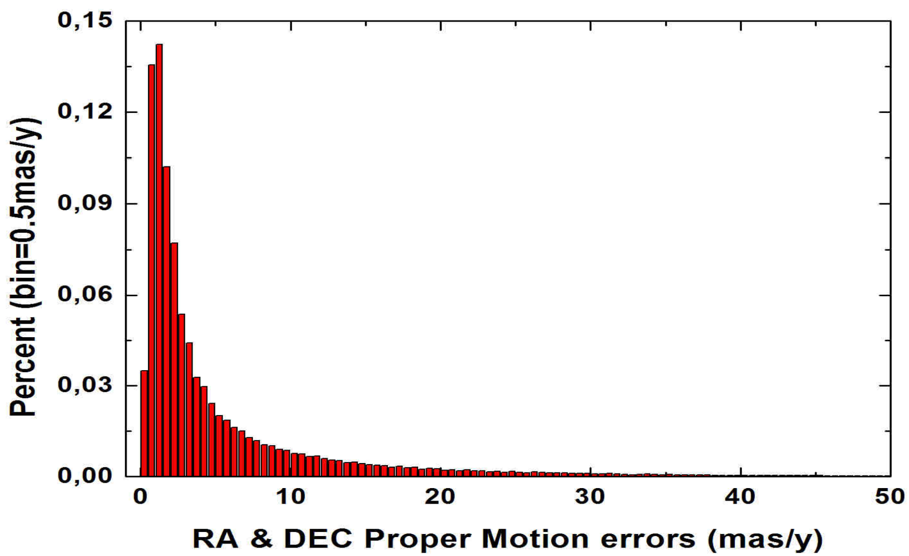

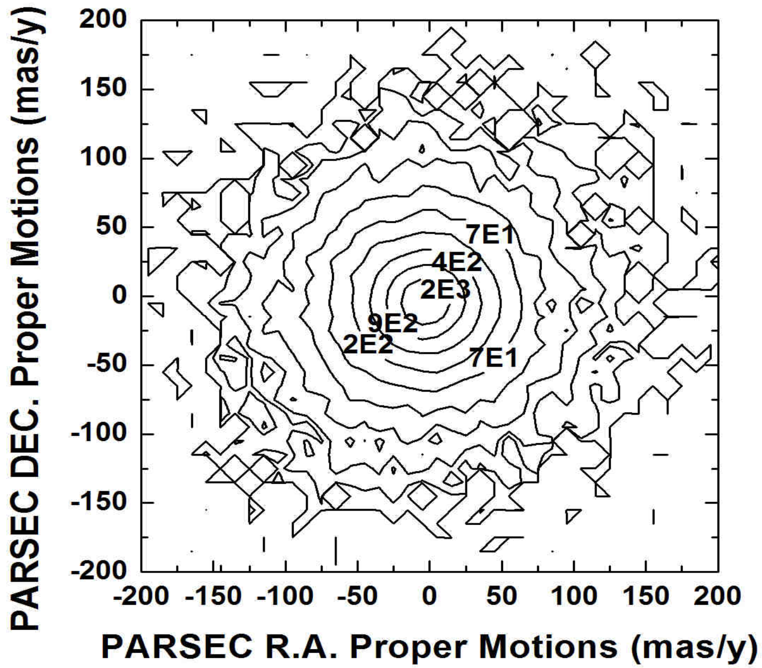

Full Program observation map

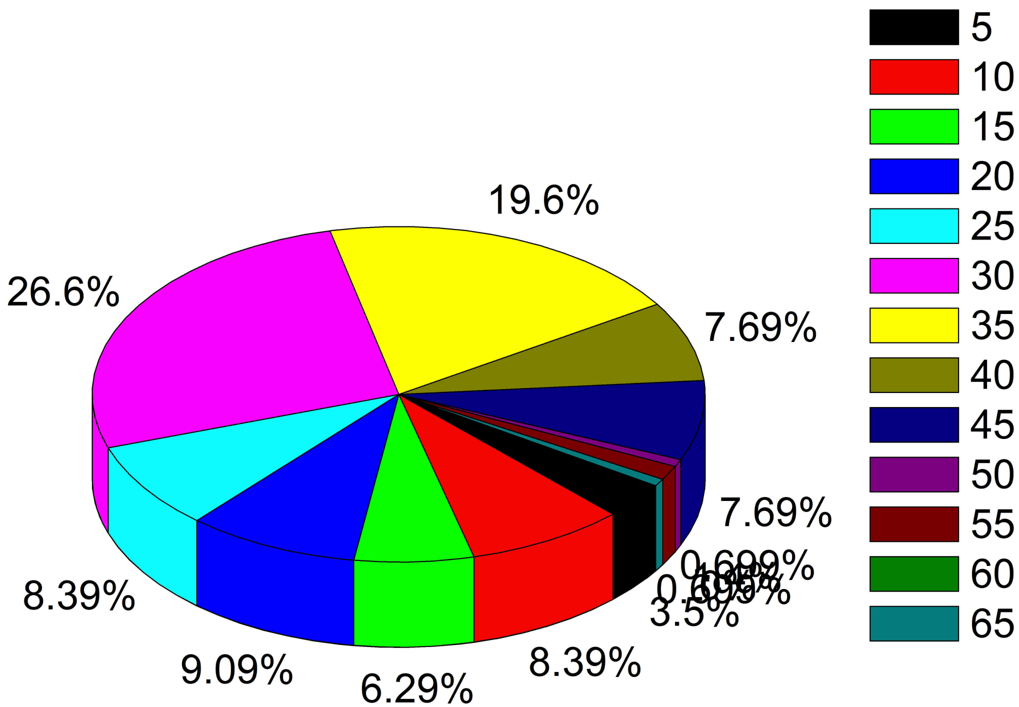

- **Out of the 143 targets, just 4 were observed around only 1 revolution; and 9 around 2 revolutions.**
- **From L0 to T7 no sub-class had more than 1 element with observations within only 1 revolution.**

- The color scheme indicates the number of observations. On the edge of the slices are the percent of sources observed those many times..

Main Output

- **More than 100% increase of L dwarfs with trigonometric parallaxes**

√ checked – preliminary parallaxes for all targets with observations spread over 3 or more years, and at least 2 independent points of the parallactic ellipse in each year – totaling 120 parallax determinations.

- **Increment to at least 10 (in conjunction with published results) the number of objects per spectral sub-class in the range L0 to T7**

√ checked – no sub-class remained underrepresented.

- **Study the binarity fraction of brown dwarfs**

√ checked – two targets examined; a IPERCOOL task force will fully address the issue for the whole program.

- **Single out interesting/benchmark objects for extended spectroscopic observation**

√ checked – SOAR spectroscopy follow-up program run for 2.5 years, to more than 50 targets examined.

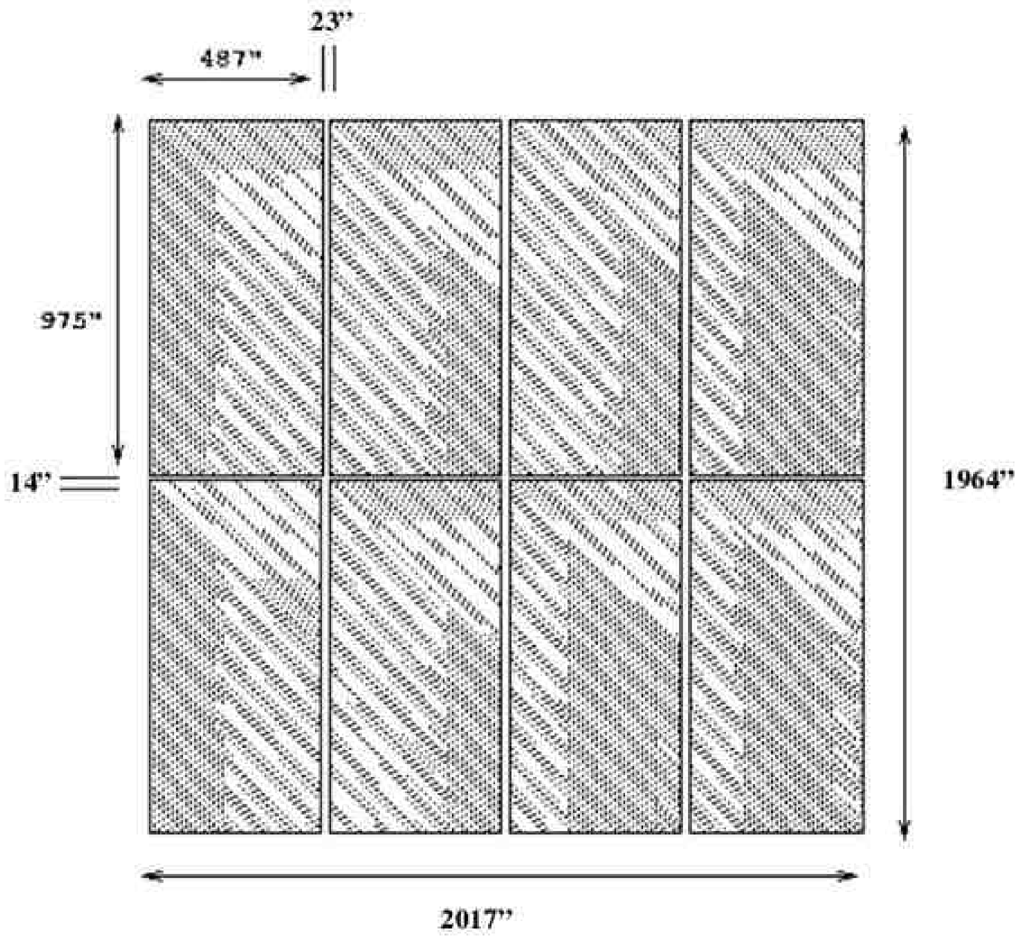

Coverage: 0.56x0.54 deg^2 (0.238 "/pix)

- ESO 2p2 WFI camera geometry, field, and pixel scale. The target always sit in CCD#7, nearby the optical axis.

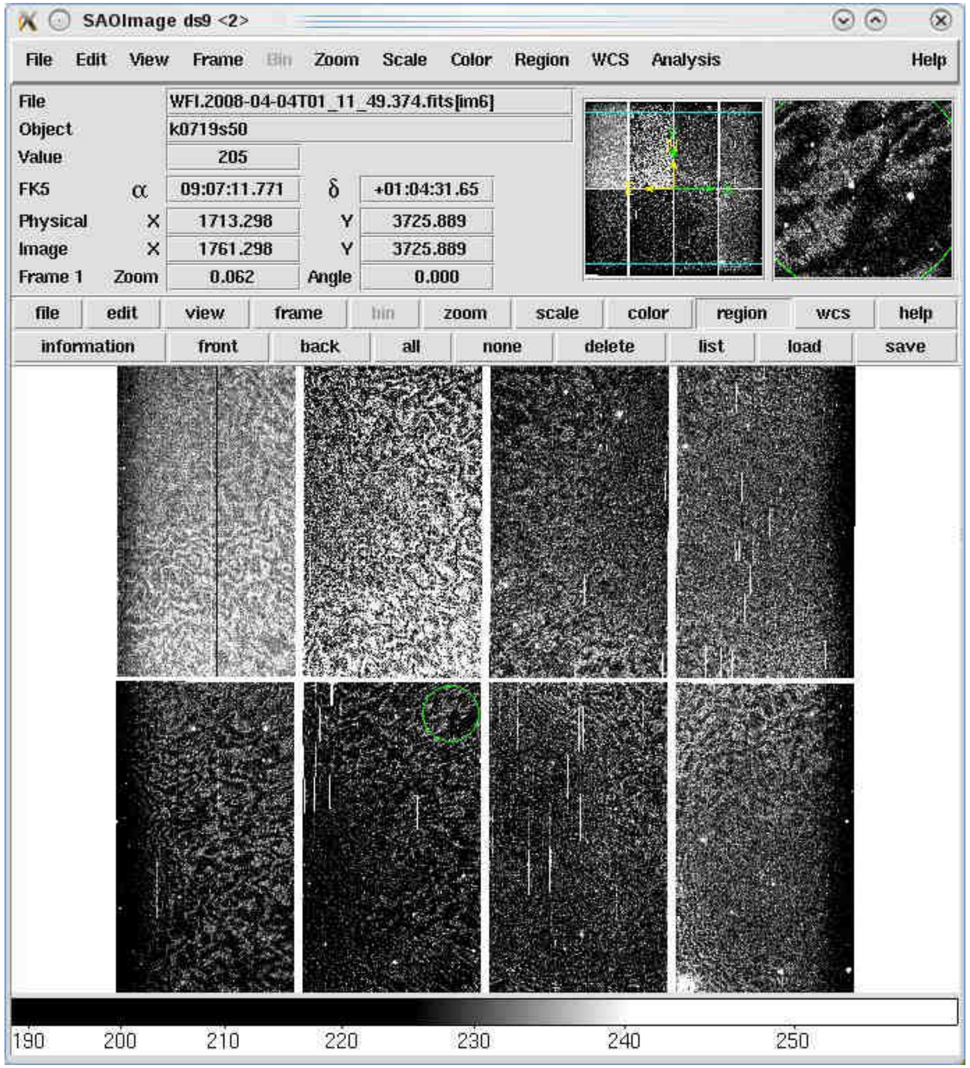

- The WFI has significant astrometric distortions but **stability** and **repeatability** are the crucial requirements for relative astrometry

- Raw image of a typical observation. The target´s spot is highlighted on the upper-left corner of CCD#7. Notice the heavy fringe pattern (due to the z-band).

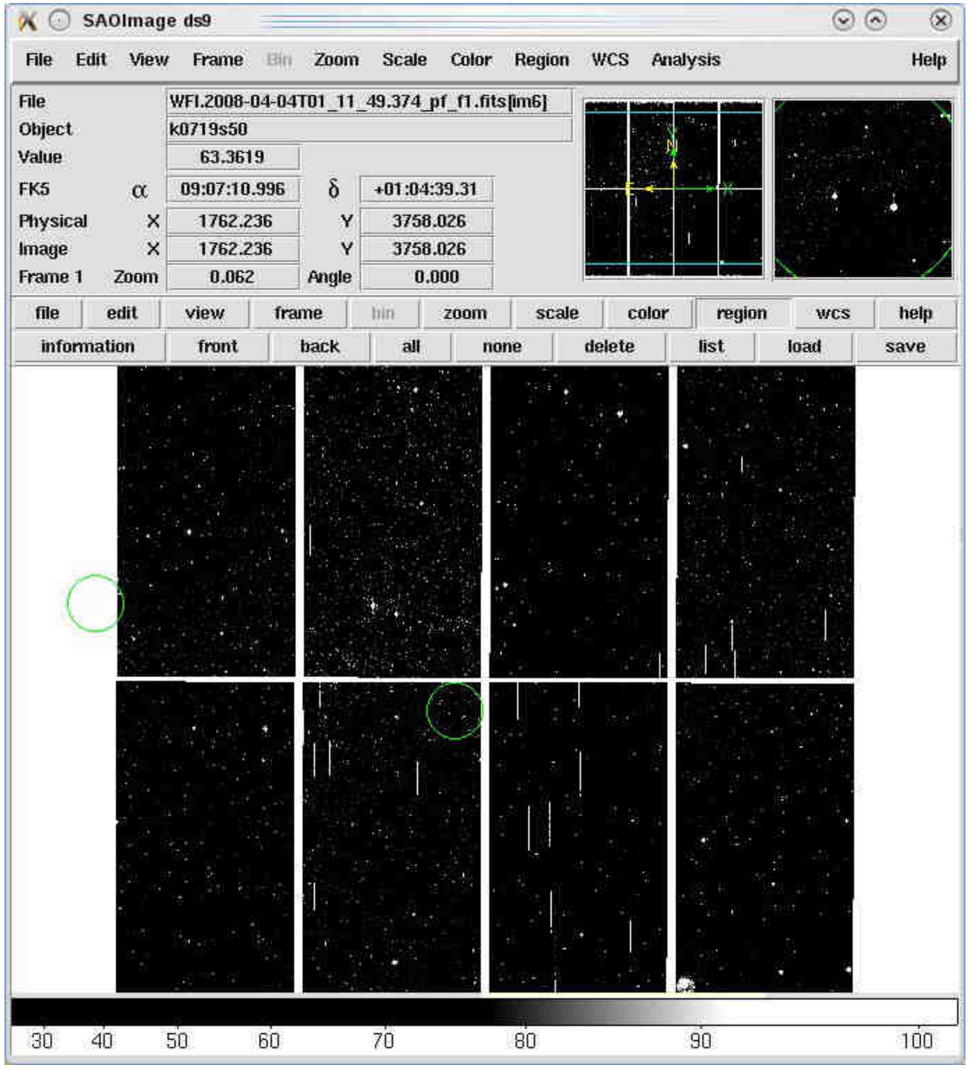

- For parallax determinations always only the top third of CCD#7 is used.
- This leads to less distortions, and further minimizes the DCR correction, which is already negligible in the z band.

- Corresponding cleaned image. Flat, bias, and a nightly fringe map correction applied. The white dots are real stars, that were hidden in the noise of the raw image.

Image Treatment

The initial image treatment uses standard IRAF routines for bias and flat. However fringe removal required a tailored approach. **The interference fringes in the infrared band images are severe, an examination of the counts shows they can vary by up to 10% over the distance of a few pixels.** Fringing is an additive effect that can be corrected making a fringe map and subtracting it from the raw images. The suggested approach is to apply a standard fringe map which is updated at periodic intervals. We found it improved our centroiding by adopting a different approach and to understand why we first consider the cause of fringing. Fringes are caused by the constructive and destructive interference of the night sky emission lines that are reflected from the bottom of the CCD silicon layer with incoming radiation. **Fringes are time and observation dependent** for a number of reasons e.g.: changes in the brightness of the night sky emission lines, changes in the thickness of the silicon layer which is a function of the temperature of the CCD, changes in the angle of incidence of the light on the CCD which is a function of flexure. **The ideal case would therefore be to make a fringe map for each image but this is not feasible. Our compromise is to make a nightly fringe map whenever possible. The general procedure to construct a fringe map is to mask out objects then build a mean map from all of the observations in a given night scaled appropriately to reveal the fringe signal.**

Image Treatment

Specifically we followed the following steps:

1. For all images we identify all the objects and make an object mask.
2. For each image we make a sky map by fitting a plane to all the unmasked pixels including a 3 clipping rejection criteria. This changes in the course of the night so it is necessary to remove it from each frame independently.
3. We select a fringe calibration image subset consisting of all the short 50s and 4 of the long science exposures. We did not include all the science images in this subset as the object mask does not always cleanly block out all of the target signal and using all the science frames with the target on the same pixel results in a ghost image around the move-to-pixel position.
4. We make a median image by scaling all subset images by the exposure time and making a median of the unmasked pixels.
5. The first fringe map is constructed by smoothing the median image using a block size of 5 pixels.
6. This first fringe is subtracted from all images providing sky subtracted and relatively fringe free observations.
7. We make a new median image scaling the cleaned subset images by the weighted mean difference between the input image and the fringe image.
8. We construct a new fringe map smoothing the median image and then apply it to all the cleaned images providing fringe-free images.

Image Treatment at a glance

• Image treatment with standard IRAF routines, but fringing removal with tailored approach.
• Variation of counts as high as 10% over the distance of few pixels are cured by generating a **nightly fringe map** built from the science frames and subtracted from each **raw frame** in two passes.
• First, the image contribution is scaled using the **exposure time**.
• Next, the **image mean counts** are used as scale factor.

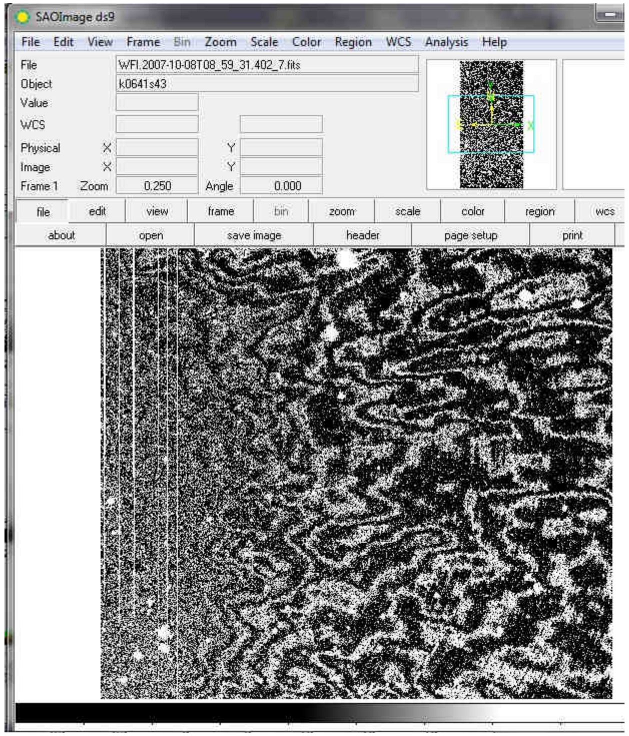

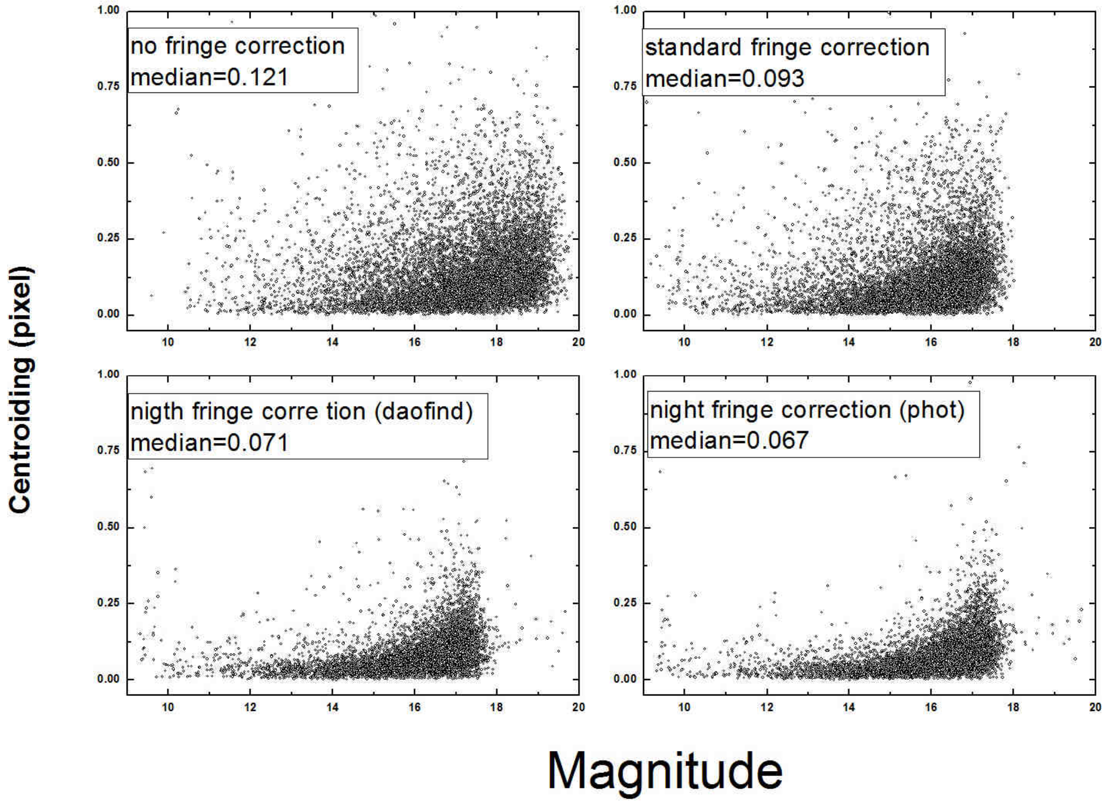

Parallaxes

On aiming to parallax precision at 5mas or better, what should translate to an error smaller than 10% over the distance, some factors are of key importance,

- centroiding method.
- astrometric solution.
- covering of the parallax ellipse.
- solution algorithm.

Parallaxes

On aiming to parallax precision at 5mas or better, what should translate to an error smaller than 10% over the distance, some factors are of key importance,

- centroiding method.
- astrometric solution.
- covering of the parallax ellipse – already taken care during the 4 years observations, every 2 or 3 months; and also a target priorities arrangement so that most of targets are very well covered.
- solution algorithm.

The Distribution of observations

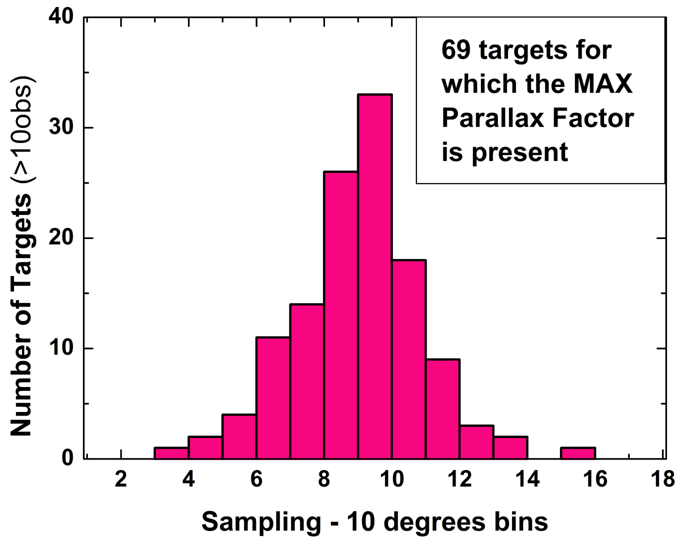

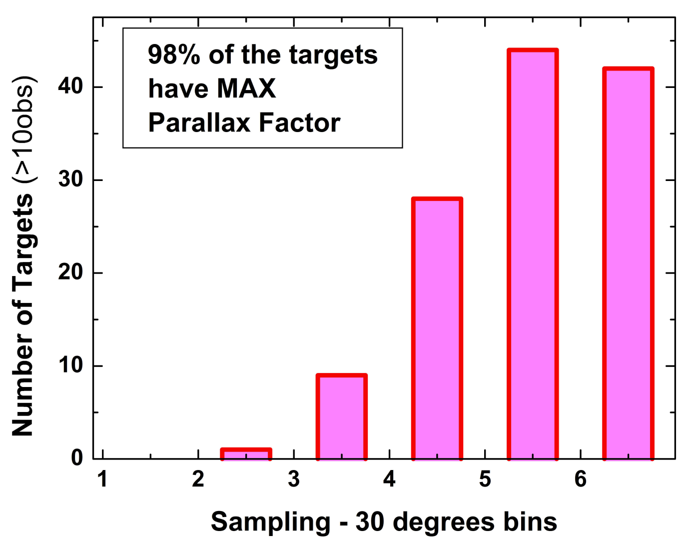

- The observations at the regions of maximum Parallax Factor are well represented, but most of the targets present the (half) parallax ellipse well sampled.

- Both features – Max Parallax Factor & good sampling of the parallax ellipse get clearer when sampling at 30deg of longitude difference.

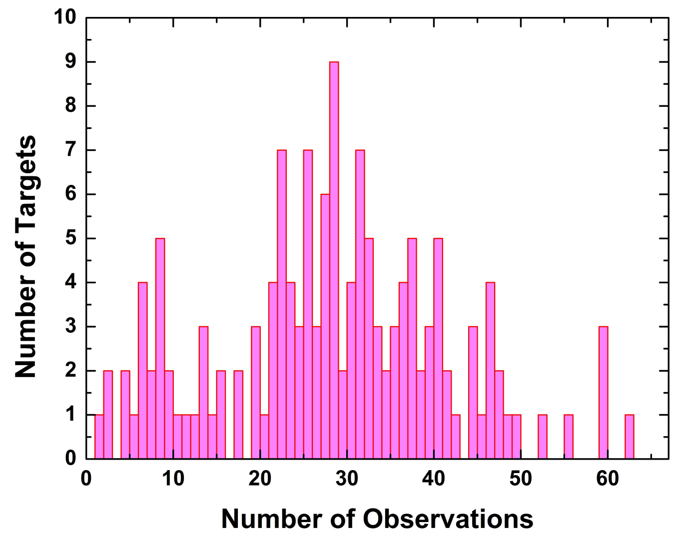

The Distribution of observations

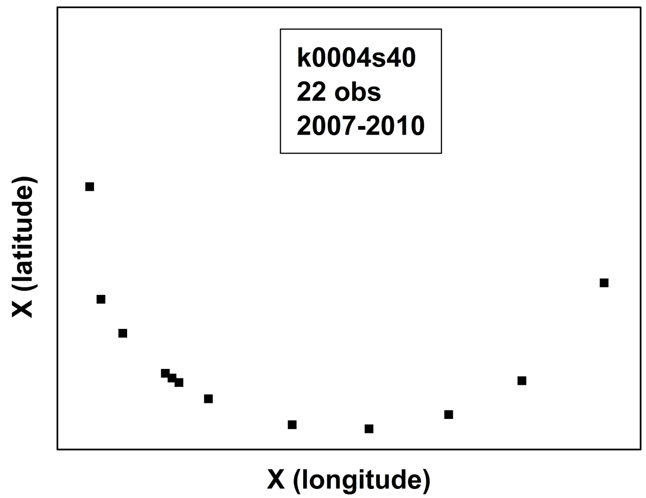

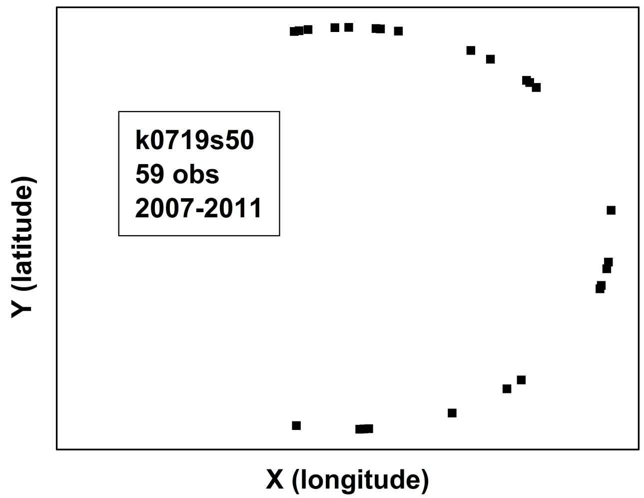

- The observations at the regions of maximum Parallax Factor are well represented, but most of the targets present the (half) parallax ellipse well sampled.
- Both features – Max Parallax Factor & good sampling of the parallax ellipse get clearer when sampling at 30deg of longitude difference.

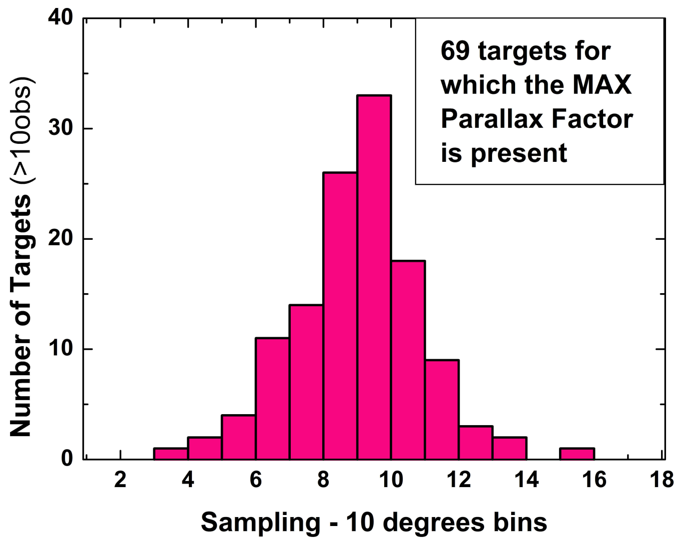

Parallaxes

On aiming to parallax precision at 5mas or better, what should translate to an error smaller than 10% over the distance, some factors are of key importance,

- centroiding method - six independent centroid determinations: the one regularly used from TOPP/OATo parallax programs; IRAF's DAOFIND/PHOT; CASU's baricenter; SEXTRACTOR's baricenter and gaussian settings; and the one from the Gaia GBOT's routines. The error based comparison between those methods shows negligible differences for well imaged stars, with averages ranging from 4.9mas to 7.5mas. However when all stars are include larger differences appear, the average error ranging from 7.1mas, for the CASU's centroid (which optimized for baricentric adjustment), to 27.6mas, for the TOPP's method.

- astrometric solution.

- covering of the parallax ellipse.

- solution algorithm.

Centroiding method

Catalog	Solution	$\lvert\Delta\alpha\cos\delta\rvert$ (mas)	E(α)	$\lvert\Delta\delta\rvert$ (mas)	E(δ)	$\lvert\Delta\rvert$ (mas)	E(Δ)
UCAC	phot	152.5	16.1	151.2	15.9	151.9	16.0
PPMXL	pr3	91.9	10.3	109.3	10.9	100.6	10.7
PPMXL	rwf	148.0	15.6	178.4	17.8	163.1	17.2
PPMXL	rr5	196.8	18.4	189.7	18.0	193.3	18.2
PPMXL	se2	134.8	14.3	139.7	14.3	137.3	14.3

- **phot** – from IRAF: enhanced centroid task.
- **pr3** – from GBOT: astrometry driven; wings and skewness are taken into account through an initial determination of the centroid by marginal X,Y projections. baricenter performed on a tight retangular window.
- **rwf** – from CASU: photometry driven; 2 sequential steps of local background removal; initial clipping run to un-weight pixels with discrepant counts; baricenter finally applied; 2D regular, linear fitting-apt components of the image are accessed.
- **rr5** – from TOPP: astrometry driven; unweighted bi-densional gaussian fit, although assign zeroweight to pixels which count approached the CCD nominal saturation limit; psf model dominates.
- **se2** – from SEXTRACTOR: astrometry driven; baricenter performed over a gaussian defined window; summation performed relatively to the spatial minima, skewness and large wings are assumed constant over the astrometry field or of minor importance, as such the peak is well determined.

Centroiding method

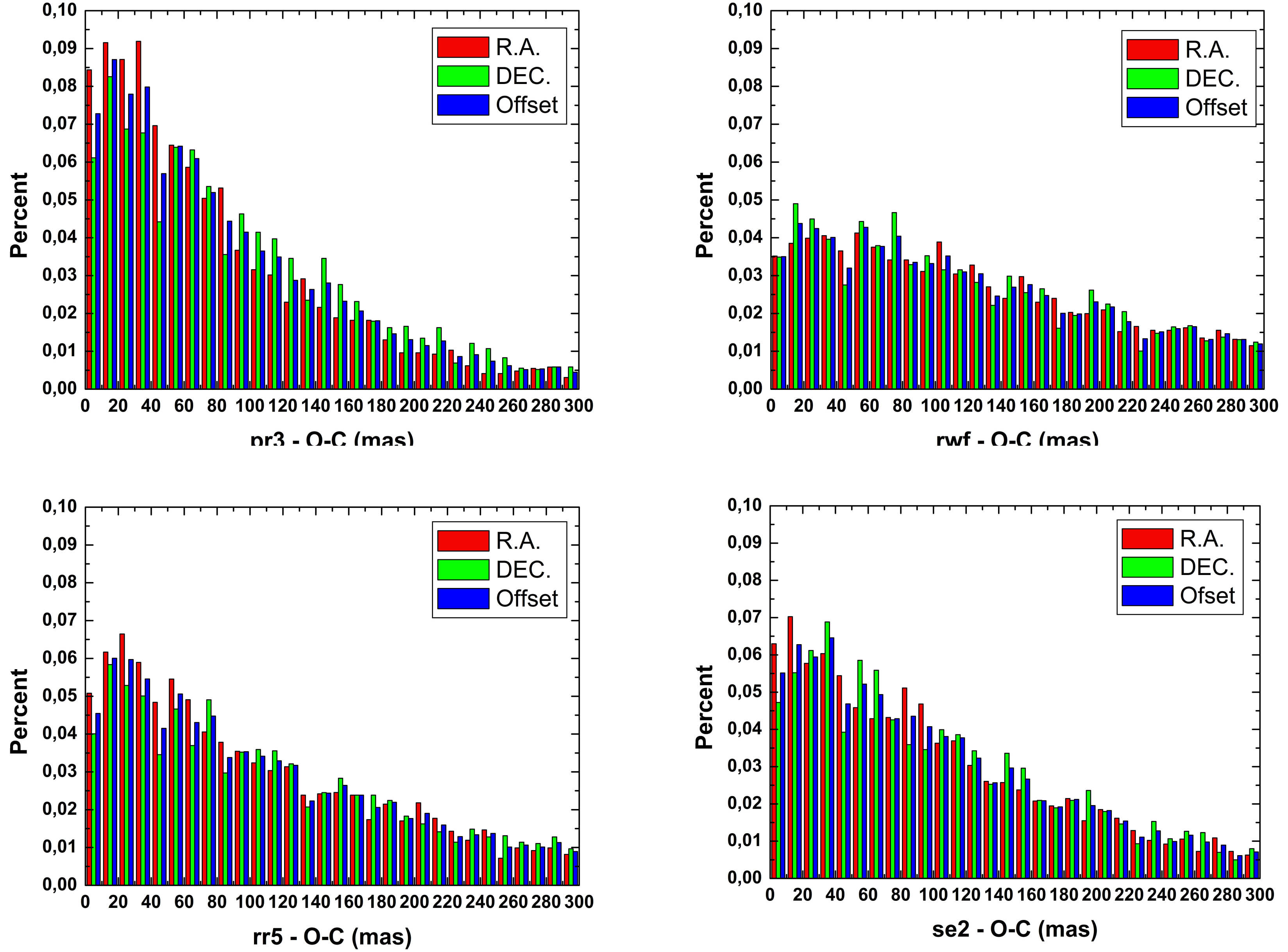

Centroiding method

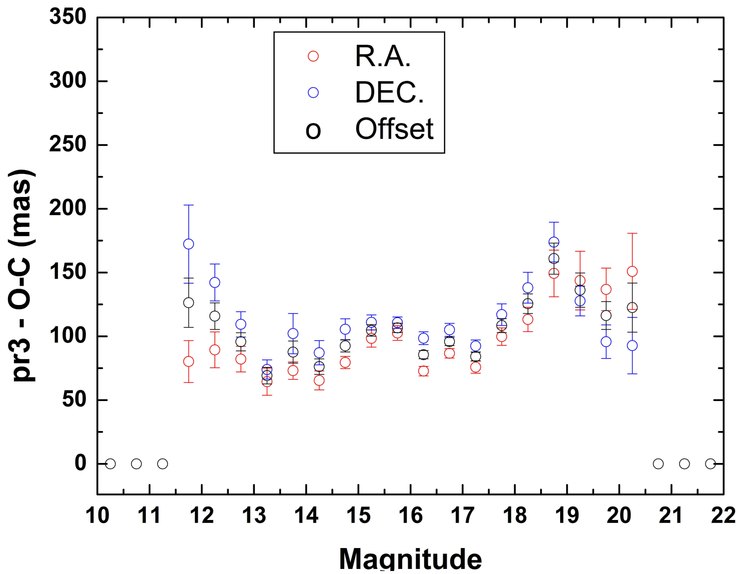

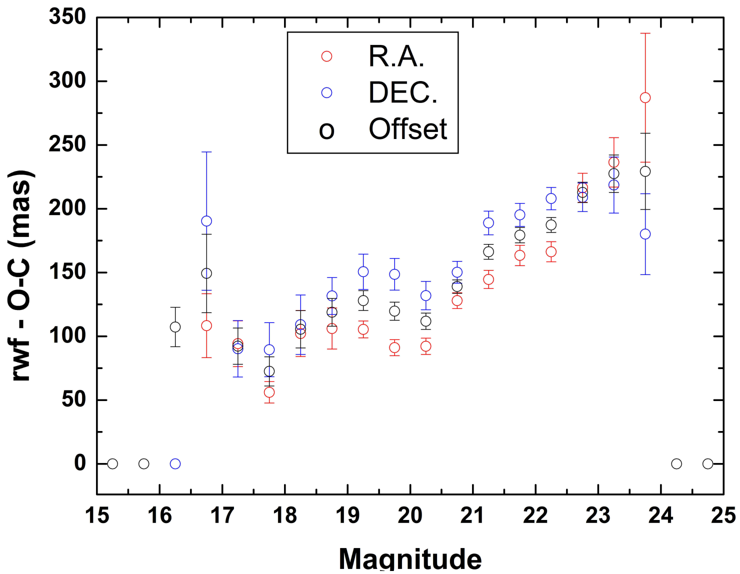

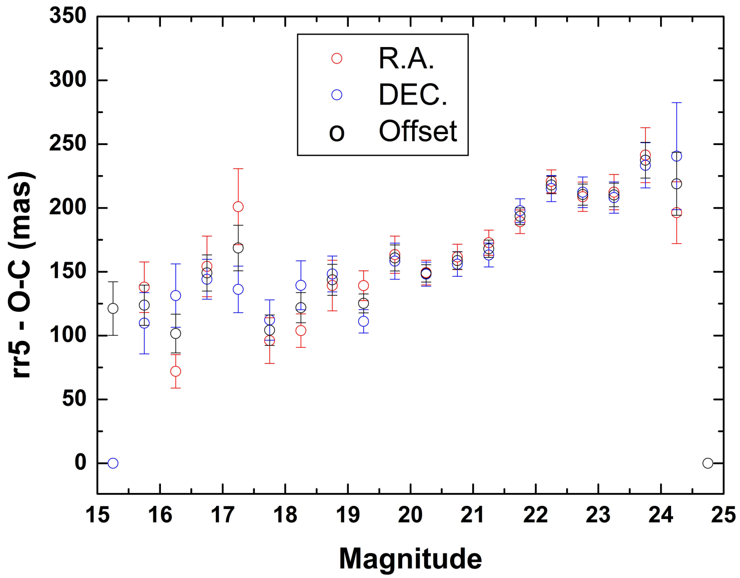

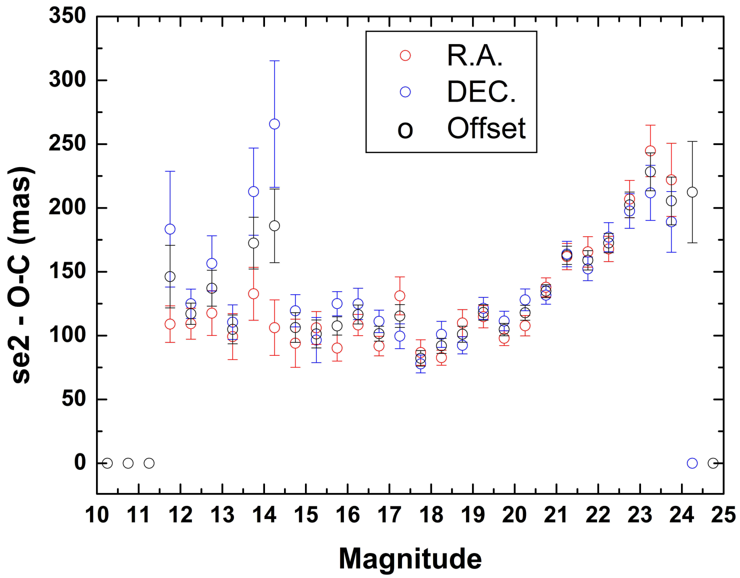

Centroiding method - adopted average centroid

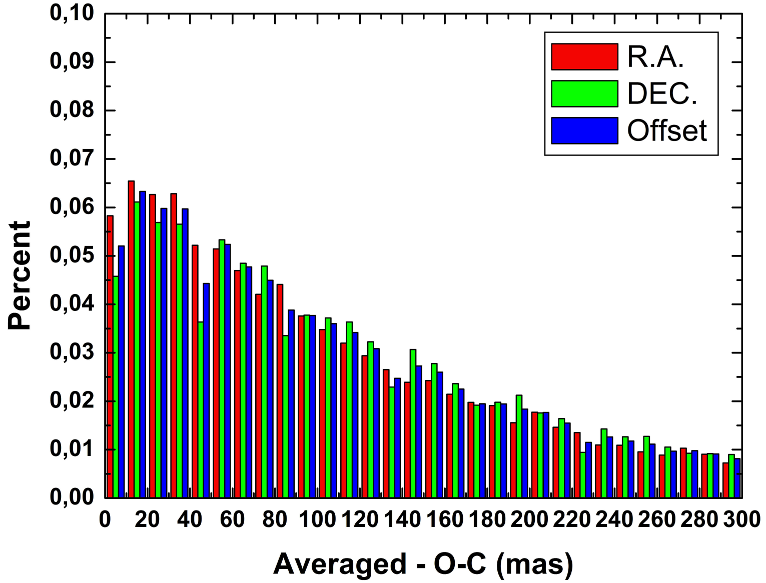

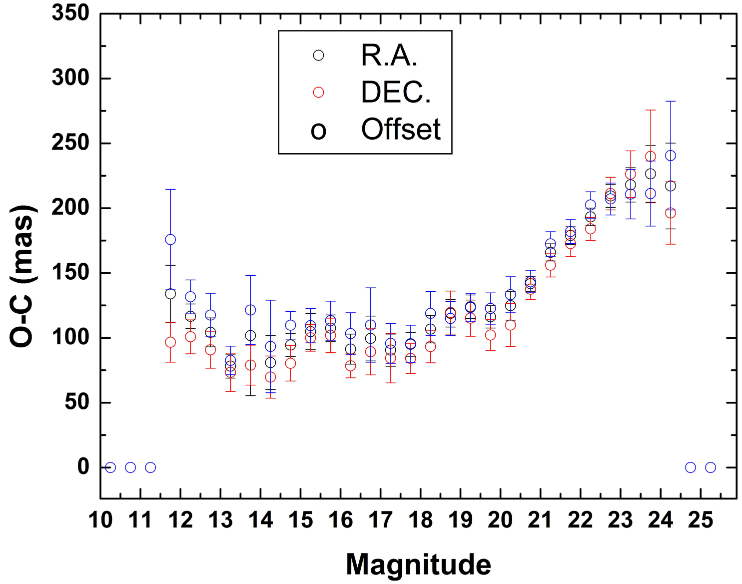

- Considering that:
- The four centroidings obtained have previously refereed methodology discussion and astrometric applications;
- Also on our sample the four centroindings offer comparable astrometric results;
- The four centroidings define each one conceptually different and independent assessment of the centers of any given star, at any given magnitude, any given state of the detector sensitivity, and at any given sky condition;
- Our results are obtained by averaging the solutions coming from the four independent measufrements – **of the same observations**.

Parallaxes

On aiming to parallax precision at 5mas or better, what should translate to an error smaller than 10% over the distance, some factors are of key importance,

- centroiding method.

- astrometric solution - always relatively to the PPMXL catalog, and on the top third of CCD7 to enable a simple polynomial mapping function. After obtaining consistent sets of standard coordinates (ξ , η), the combination of the sets (i.e., observations) is approached in 3 different ways embedded in the solution algorithms.

- covering of the parallax ellipse.

- solution algorithm.

Astrometric Solution - Catalogs

• The former solutions (Andrei et al., 2011, 2013) used respectively the UCAC2 and UCAC4 as base catalogs.
• **Both fully cover the south celestial hemisphere, for R magnitudes of about 7.5 to 16, resulting on an average star density of 0.76 star per square arc-minute**. The observed positional errors are about 20 mas for the stars in the 10 to 14 magnitude range, and about 70 mas at the limiting magnitude of R ~16 .
• For the current solution the PPMXL is employed as base catalog. This is done both to substantially multiply the number of reference stars, as well as for practical reasons due to matching difficulties between the various centroid solutions available.
• The PPMXL is a catalog of positions, proper motions, 2MASS and optical photometry of 900 million stars, aiming to be complete down to about V=20 full-sky. **The resulting average stellar density is 6.06 stars per square arc-minute. The mean errors of positions at epoch 2000.0 are 80 to 120 mas, if 2MASS astrometry could be used, 150 to 300 mas else**.

• The following table of observed-minus-calculated (OC) averages shows that there is no loss for the astrometric solution by adopting the PPMXL.

Astrometric Solution - Catalogs

Catalog	Solution	$\lvert\Delta\alpha\cos\delta\rvert$ (mas)	$E(\alpha)$	$\lvert\Delta\delta\rvert$ (mas)	$E(\delta)$	$\lvert\Delta\rvert$ (mas)	$E(\Delta)$
UCAC	phot	152.5	16.1	151.2	15.9	151.9	16.0
PPMXL	pr3	91.9	10.3	109.3	10.9	100.6	10.7
PPMXL	twf	148.0	15.6	178.4	17.8	163.1	17.2
PPMXL	rr5	196.8	18.4	189.7	18.0	193.3	18.2
PPMXL	se2	134.8	14.3	139.7	14.3	137.3	14.3

Astrometric Solution - Objects Matching

Matching – The probability of correct matching of one object in two frames is
$P = 1/(\Phi S)$, *where Φ is the stellar density and S is the frame size.*

Usual cone search strategies run into trouble for long time intervals. We avoided such pitfalls by adopting the following strategy:

1. because of moving-to-pixel telescope pointing and double exposures, unpaired objects are assigned low order in the matching process.
2. assigning high order in the matching process to objects with no proper motion between the first two nights.
3. using relative astrometry precise to better than 100mas, under those conditions P is larger than 0.99 already when the third night is added even for Φ=1000/deg2.
4. removing the stars matched in the previous step Φ drops dramatically, and the process re-starts taking stars with smallest proper motions.
5. finally the objects unpaired in the first step, and cases of suspicious magnitude or position matching are considered, now allowing for periodical jitter.

- The pipeline converges rapidly, has shown to be robust during artificial and surveyed tests, and is effective to sign out binary candidates.

Astrometric Solution - Objects Matching

Fitting – **Before start the matching process all frames must be placed onto a common reference frame.** Instead of the usual choice by the first or densest frame as reference we opted to build a mean frame. The mean frame is build by step-wise polynomial adjustment of time close frames. **We simulated the observation of a patch of the sky observed twice along 26 nights with up to 800 stars, mimicking a typical PARSEC set.** Using a gaussian noise generator stars appeared or not in each frame, centroid errors were assigned, plus terms of tilt and telescope pointing. **The table below summarizes the results obtained taking as reference frame either the first frame of the sample, or the densest, or finally the mean frame – which is clearly the optimal choice. The building of the mean frame, though asking for an additional computational effort, saves steps when later matching the objects.**

Solution	Stars Matched	Mean Precision (mas)
1st frame	257 ± 76	0.0028
Densest frame	493 ± 128	0.0026
Mean frame	527 ± 134	0.0023

Parallaxes

On aiming to parallax precision at 5mas or better, what should translate to an error smaller than 10% over the distance, some factors are of key importance,

- centroiding method.
- astrometric solution.
- covering of the parallax ellipse.
- solution algorithm – the unknowns can be grouped by

$$\boxed{\xi_0 + \mu_\xi \Delta t + \pi P_\xi - x - (ax + by + c) = 0}$$

which forms a linear system of observation equations involving astrometric and instrumental parameters. In the absence of other astronomical knowledge or assumption, the system is rank deficient. Three methods are used to solve for the parallax. The parallaxes are rendered absolute by applying a galaxy model correction

Parallaxes – Iterative Gauss-Seidel Algorithm

• A base frame is defined, usually the first one well observed, since the number of stars is not a hindrance given the quality of the instrument and site.
• The other frames are referred to the based frame by using the common stars for solving for the unknowns *A*, *B*, *C* in

$$\boxed{\xi_{\mu,\nu_0} = A_\nu x_{\mu,\nu} + B_\nu y_{\mu,\nu} + C_\nu}$$

• the relations are analogous in η. In solving for the unknowns the target star is not used, but this normally is trascurable.
• It is implicit that proper motion and parallax terms are not important, or that the stars for which they do are expelled from the plate adjustment process. This does not affects the determination of the A, B, C unknowns.
• With all standard coordinates (ξ , η) set on the base frame, the astrometric solution can be solved for

$$\boxed{\xi_{\mu,\nu} = \xi_{\mu,\nu_0}(1.0 + a_\mu) + (t_\nu - t_{\nu_0})\mu_\mu + (P_{\xi_\nu} - P_{\xi_{\nu_0}})\omega_\mu.}$$

• The parallax factors are determined from the best available values for the Earth coordinates (X,Y,Z).
• On determining the proper motions and parallaxes, the process can iterate or elevated the degree of the polynomial adjustment to the base frame – but practice shows that this was usually not necessary in the PARSEC program, due the instrumental, methodological, and observational setups.

Parallaxes - GAUSSFIT least-squares robust estimation

• The canonical approach is to express the stellar motions in equatorial standard coordinates and to build a system of equations which includes the astrometric parameters of all stars and the instrumental parameters of all frames, the latter suitably modeled by a first order polynomial. In so the observation equation for the longitudinal standard coordinate of a generic star on a frame *i* reads:.

$$
-x_i = a_i x_i + b_i y_i + c_i - \xi_0 - \mu_\xi (t_i - t_0) - P_{\xi_i} \pi_\xi
$$

• Above, (x_i, y_i) are the object's image centroid, t_0 a chosen reference epoch and P_ξ the parallax factor. The parameters to be estimated are ξ_0 , μ_ξ, , π_ξ i.e., the star position at t_0, its longitudinal proper motion and its parallax, and the instrumental coefficients a, b, c mapping each frame onto the tangential plane.

• The intrinsic rank deficiency of this problem is tackled by using a direct approach requiring nine additional constraints to fix the solution.

$$
\sum \xi_{0i} = \sum \xi_{CAT_i} ; \sum x_i \xi_{0i} = \sum x_i \xi_{CAT_i} ; \sum y_i \xi_{0i} = \sum y_i \xi_{CAT_i}
$$

$$
\begin{gathered}
\sum \mu_i = 0; \sum x_i \mu_i = 0; \sum y_i \mu_i = 0 \\
\sum \pi_i = 0; \sum x_i \pi_i = 0; \sum y_i \pi_i = 0
\end{gathered}
$$

• This choice corresponds to fix the astrometric parameters relatively to the baricenter assumed at still. It orthogonalizes the astrometric parameters of the reference stars with respect to the instrumental parameters.

Parallaxes - Direct ellipse fitting

• As the starting point a mean frame is build using the step-wise polynomial adjustment of time close frames and the matching by hierarchical cone search.
• Next the ecliptic standard coordinates (ξ'_i , η'_I) at t_i epoch of observation of the target star are derived.
• Hence (ξ'_i , η'_I) can be fitted with an elliptic motion modeling the parallactic effect superimposed to a linear term which accounts for the star's transversal motion as

$$\boxed{\xi_{t_i}(x,y) = \pi_\xi sin(t_i + \phi_\xi) + \mu_\xi(t_i - t_0)}$$

• Above, π_ξ is the target's parallax, Φ_ξ is a phase term, μ_ξ is the longitudinal proper motion and t_0 the epoch of the mean frame. And analogously for the η' component.
• The effect of Earth's eccentricity is disregarded, given the typical distances of our targets. It can be in principle computed and corrected for being a purely geometrical effect. Nevertheless a computation of the differences for 3 fictitious stars at 20pc, and with ecliptic latitude *b*= 0°, 45°, 90° , sampled from 4 to 9 times along 6 months covering the span of the year (or of ecliptic longitudes), adjusted to a "parallactic" ellipse shows no contribution larger than 10exp-8 arcsec to the parallax.

.

Results - comparison of methods

• As an example, we report the reduction of 6 years of observations (93 frames, 54 reference stars) of the high proper motion star LHS3482 (2MASS J19462386+3201021) with the three techniques giving very consistent results, as shown in Table.

• It can be noted that the quoted errors are sensibly smaller in the case of the direct method. An explanation could lie in the fact the standard deviations coming from the covariance matrix are slightly underestimated, while in the other two cases, the errors are estimated from the residuals of the fit to the target's trajectory and could be more realistic indicators of the true errors.

Method	π (mas)	$\mu_\alpha\ cos\delta$ (mas/y)	μ_δ (mas/y)
Block interative	68.7 ± 4.0	458.8 ± 1.2	-391.2 ± 2.0
Direct LS	68.9 ± 0.8	457.5 ± 0.2	-390.4 ± 0.3
Ellipse fit	70.0 ± 3.2	467.7 ± 0.7	-392.0 ± 1.7

Results - Proper Motions

- From the first 18 months of the PARSEC observations, it was formed a catalog containing proper motion determinations for 195,700 objects.
- It samples 42.3 deg of the southern hemisphere with the exception of the lowest galactic latitudes where the number of known L/T dwarfs is significantly reduced.

Reduction procedure

- reduction pipeline applied to entire mosaic of 8 CCDs
- each CCD reduced independently using UCAC2 stars
- Depending on the number of reference stars the polynomial degree was 2 or 3 and cross terms have been included. The rms errors of the solutions did not show any dependence on the type of the polynomial employed.
- nearest- neighbor match with 2MASS point source catalogue
- safety measure: p.m. determined for each observation pair and later averaged while removing deviant values

Results

- median rms error 5 mas/year
- p.m. distribution histograms in agreement with UCAC2 data

Results - Comparison with UCAC2

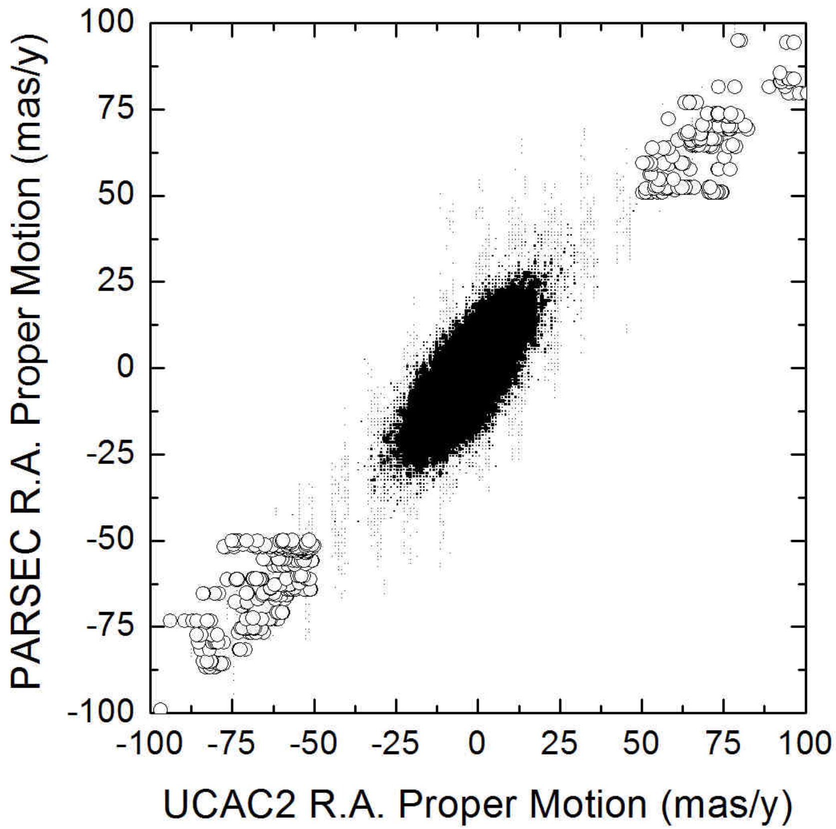

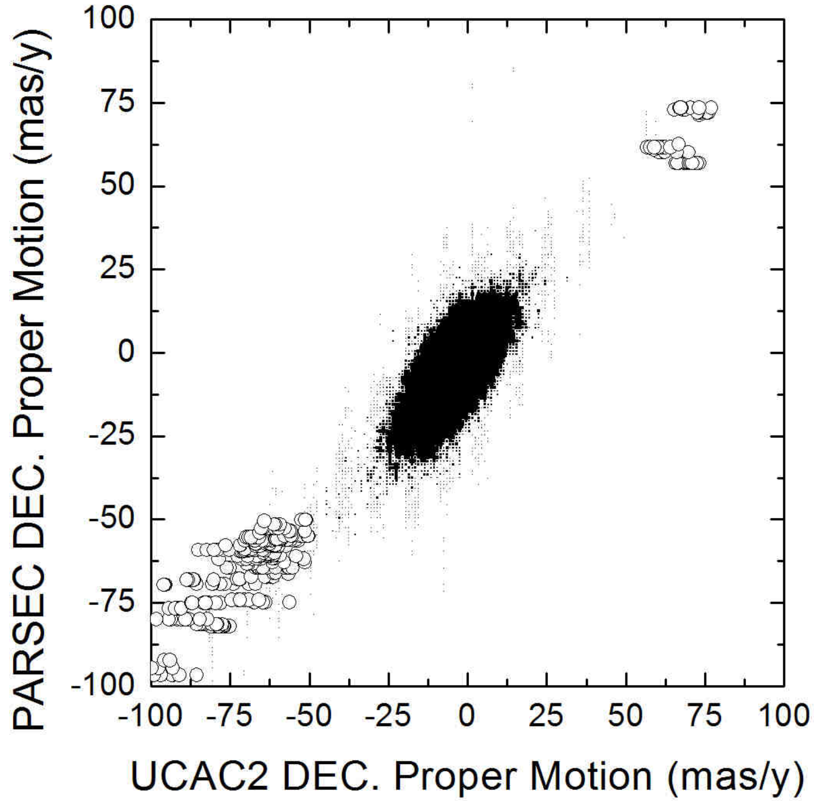

$\langle \mu_\alpha \rangle = -2.8$ mas (UCAC2 -2.7)

$\langle \mu_\delta \rangle = -4.0$ mas (UCAC2 -3.6)

Pearson's linear Correlation = 0.95 on RA and on DEC

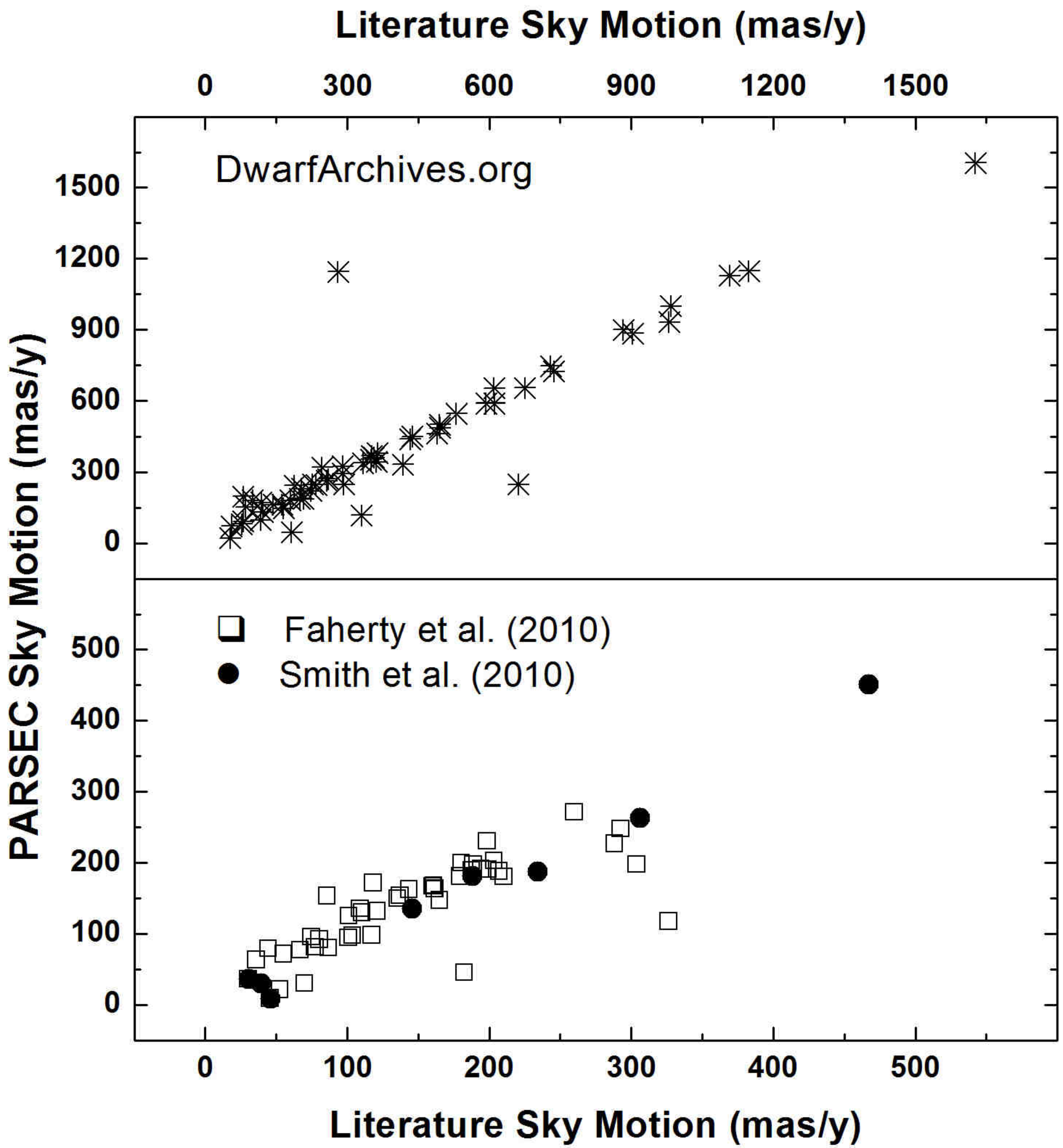

Literature Sky Motion (mas/y)
0
300
600
900
1200
1500
DwarfArchives.org
PARSEC Sky Motion (mas/y)
1500
1200
900
600
300
0
Faherty et al. (2010)
Smith et al. (2010)
500
400
300
200
100
0
0
100
200
300
400
500
Literature Sky Motion (mas/y)

Results - RPM diagram of PARSEC Proper Motion catalogue

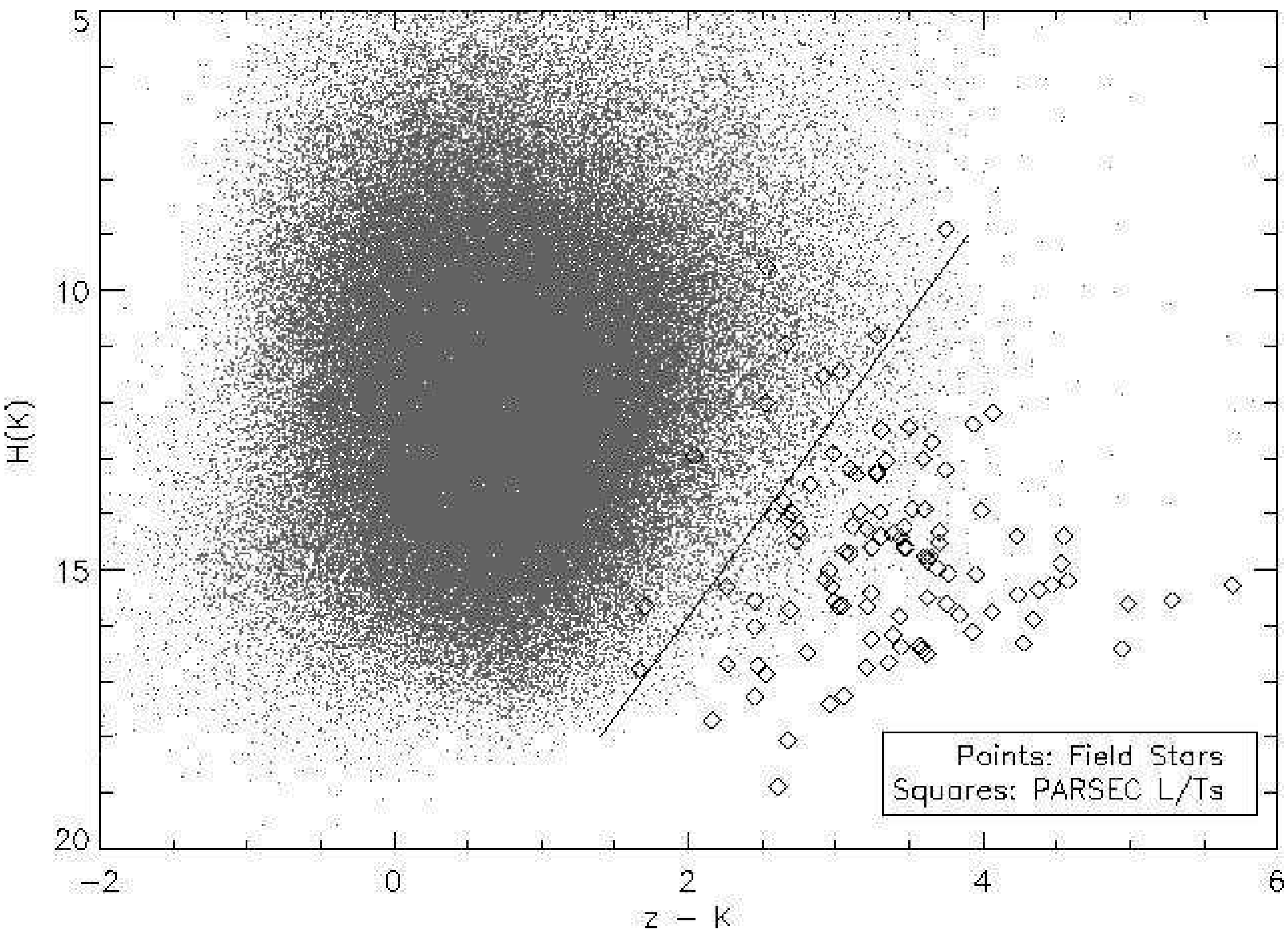

Results – Ellipse fitting, the careful formulation

• Improvements on the general ellipse fitting solution:

1- exact observation time, obliquity, and eccentricity.

2- exact ecliptic longitude.

3- numerical (exact, using the Newton's chords*) solution for the eccentric anomaly.

4- exact coefficients for the terms of parallaxe in longitude and latitude (projection of Earth's orbit on the circle of latitude).

5- tilt term to account for the angle between the apsidis and the line of solstices.

6- two free parameters to account for faulty mean position.

• The points (1) to (3) can contribute to less than 8mas (assuming a parallax as large as 1arcsec).

• The point (4) to (6) were already present before as free parameters of the general ellipse adjustment. Variation upon them would stretch the ellipse – unlikely variations of several arc-minutes would be required to create a milli-arcsec effect.

(*) acknowledgements to D.C. Andrei

Results - Ellipse fitting, the careful formulation

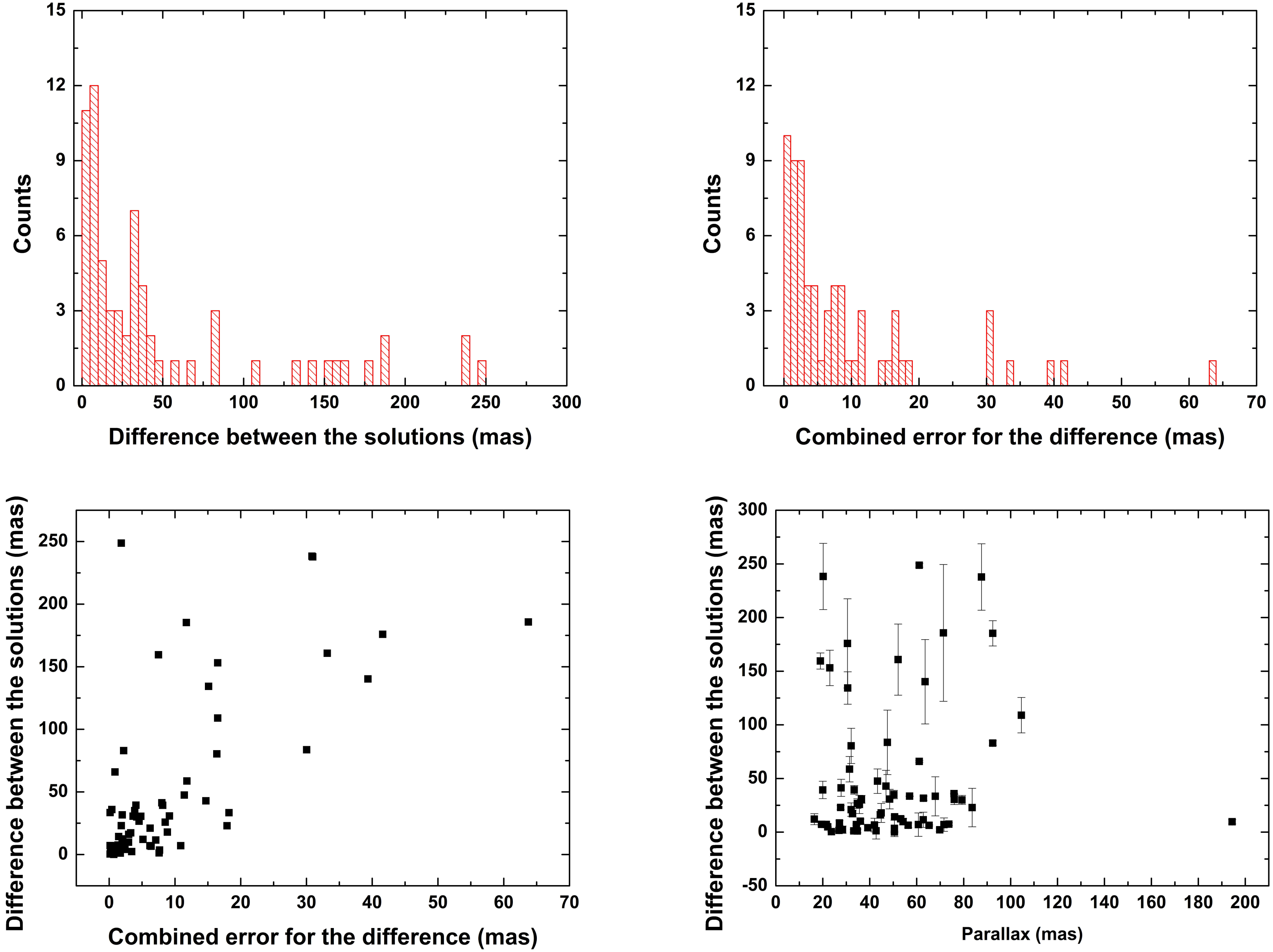

Results - Parallaxes

• On the right, simulation of 3y of parallax observations treated with the Direct LS method..

• Simulated catalog error 100mas. Simulated single measurement error 20mas. 30 Monte Carlo runs.

• From the histogram: mean π error 2.7mas and σ 6.0mas.

• Below, parallax determinations from the PARSEC program. On the left, using the Ellipse fitting method. On the right, using the Block Iterative method.

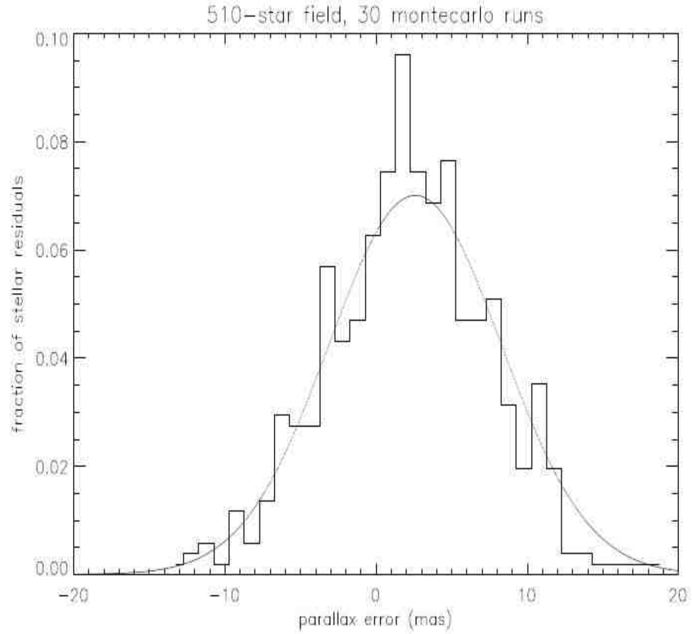

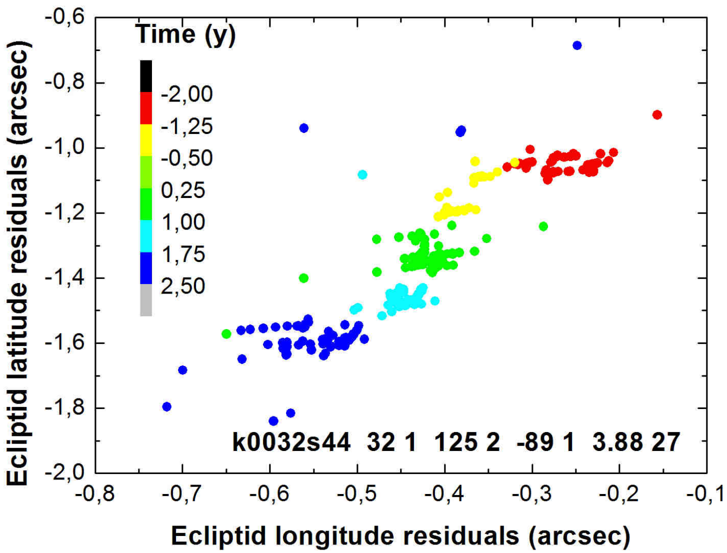

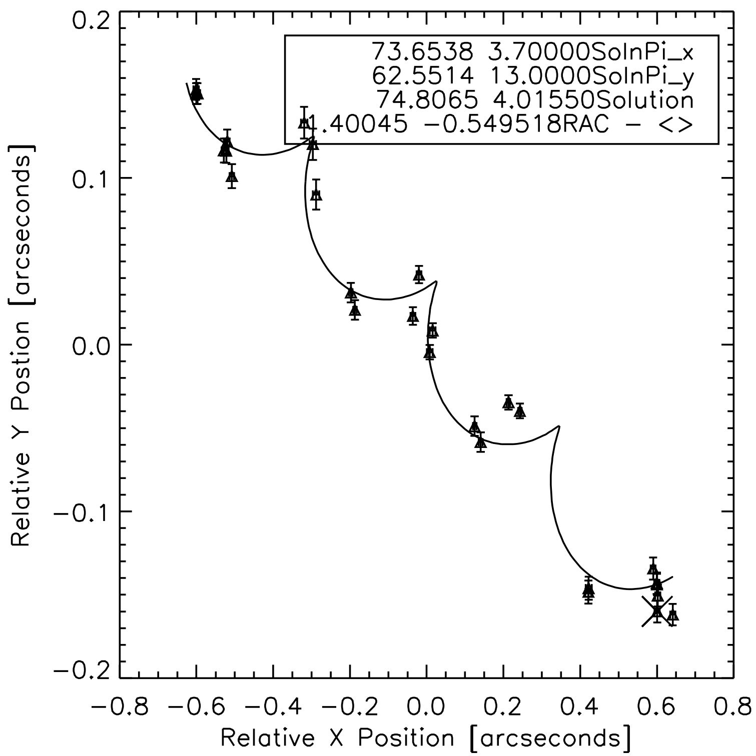

Results - Parallaxes

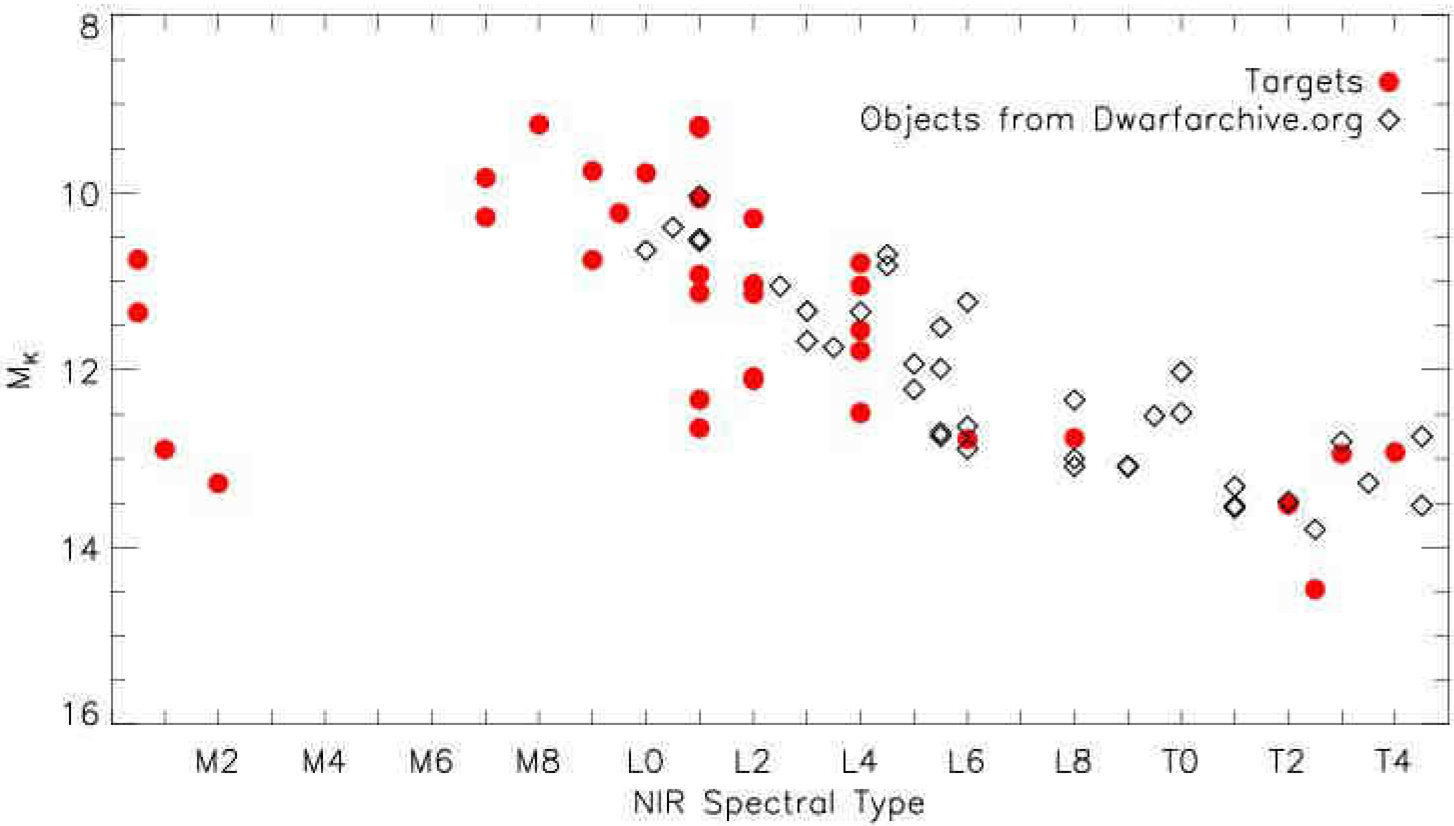

• Mk absolute magnitude derived from PARSEC parallax and the spectral type derived from SOAR spectroscopy.

• Comparison objects are also plotted illustrating the need of absolute distances from trigonometric parallax to properly model the BD mass-luminosity relationship.

Results - Parallaxes, comparisons

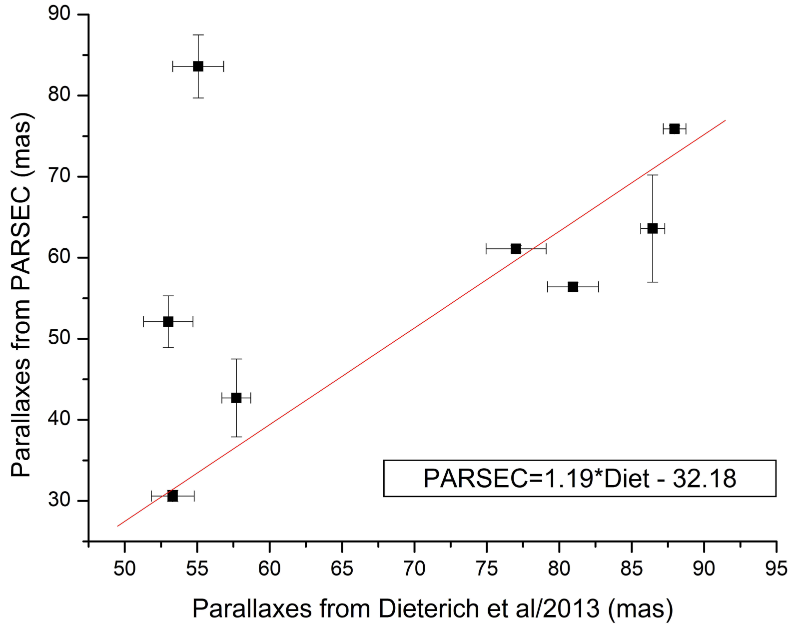

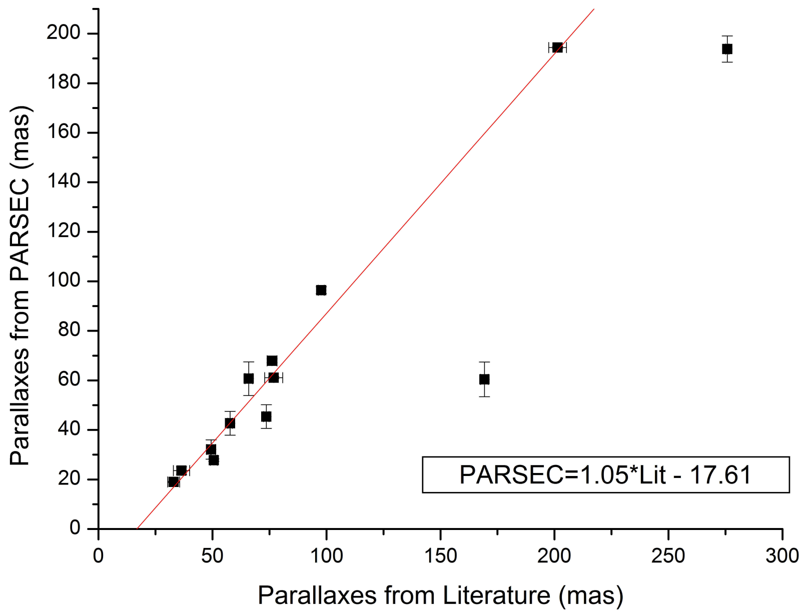

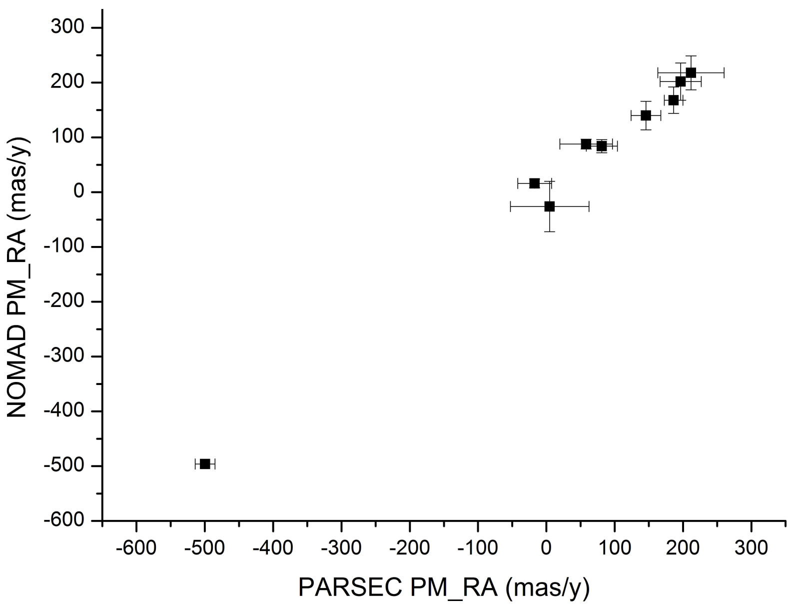

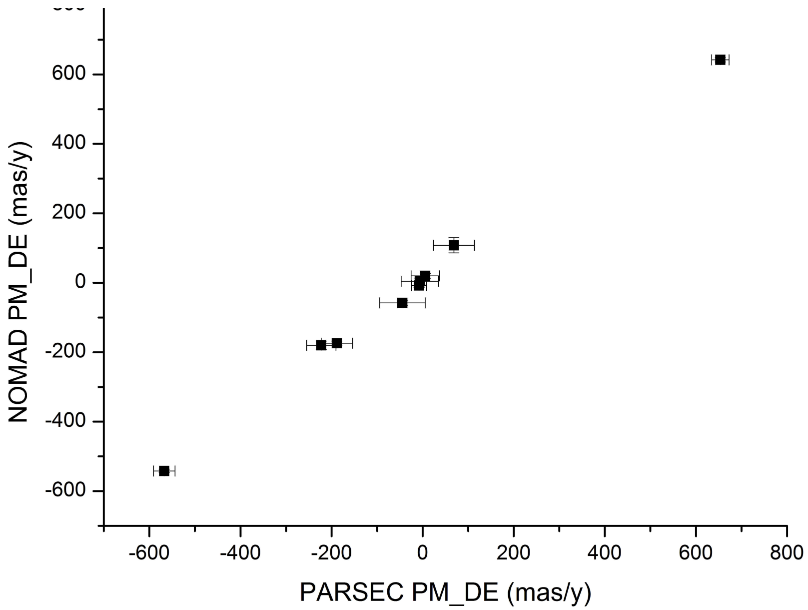

Results – Parallaxes, the Table (for 116 objects – 27 to come yet)

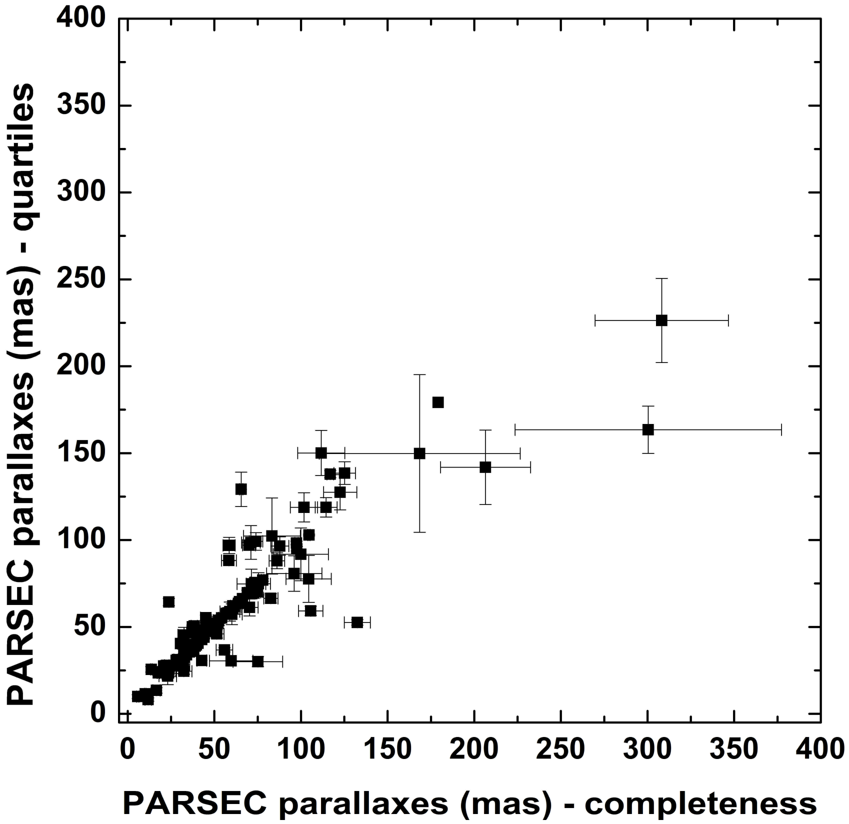

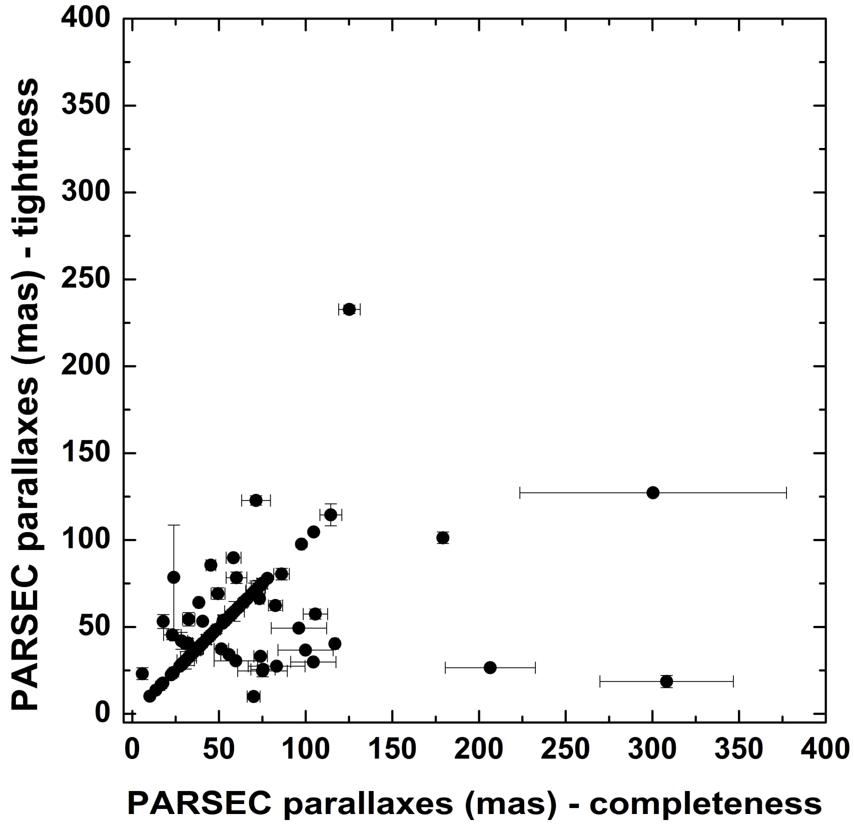

Results - Parallaxes, the Table (for 116 objects - 27 to come yet)

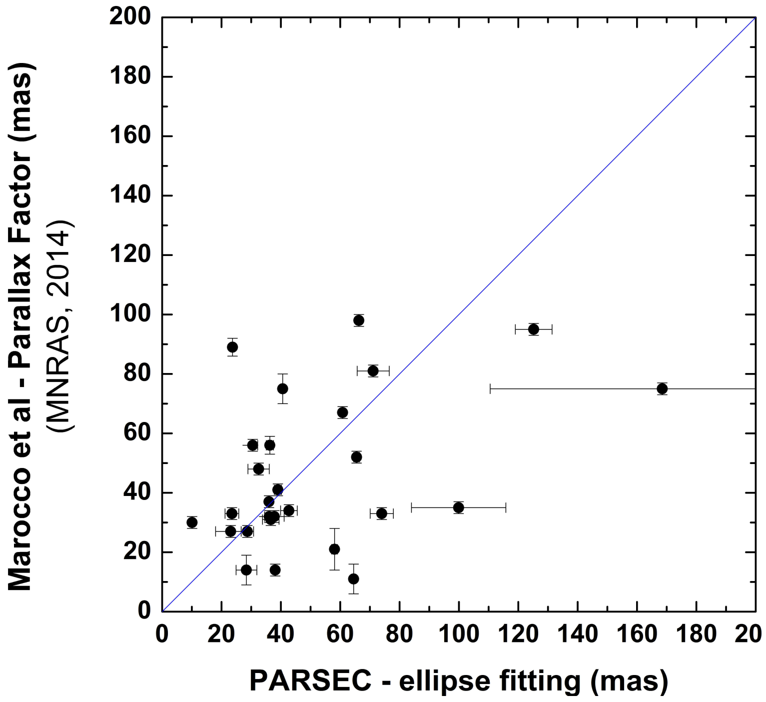

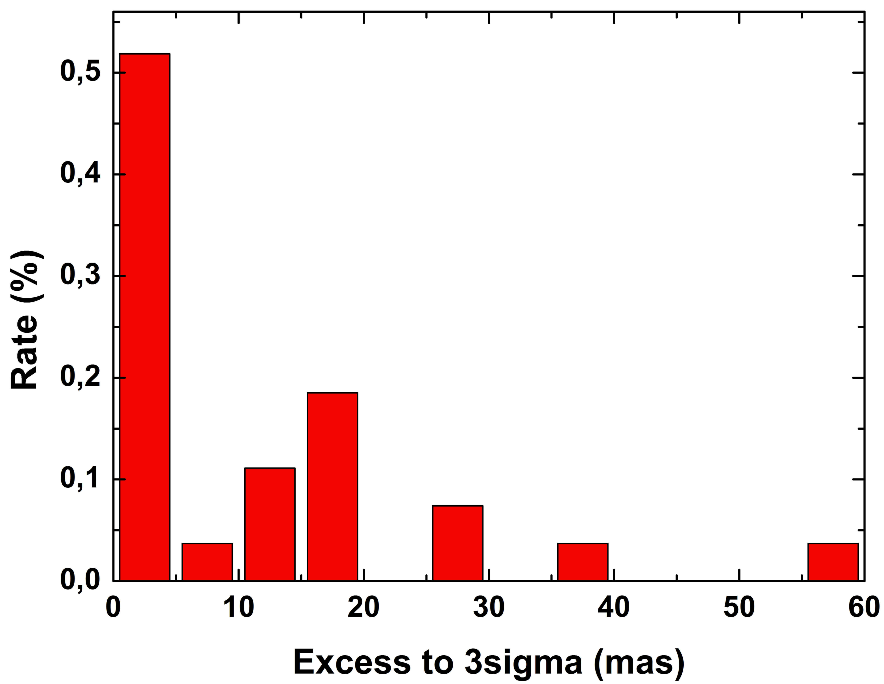

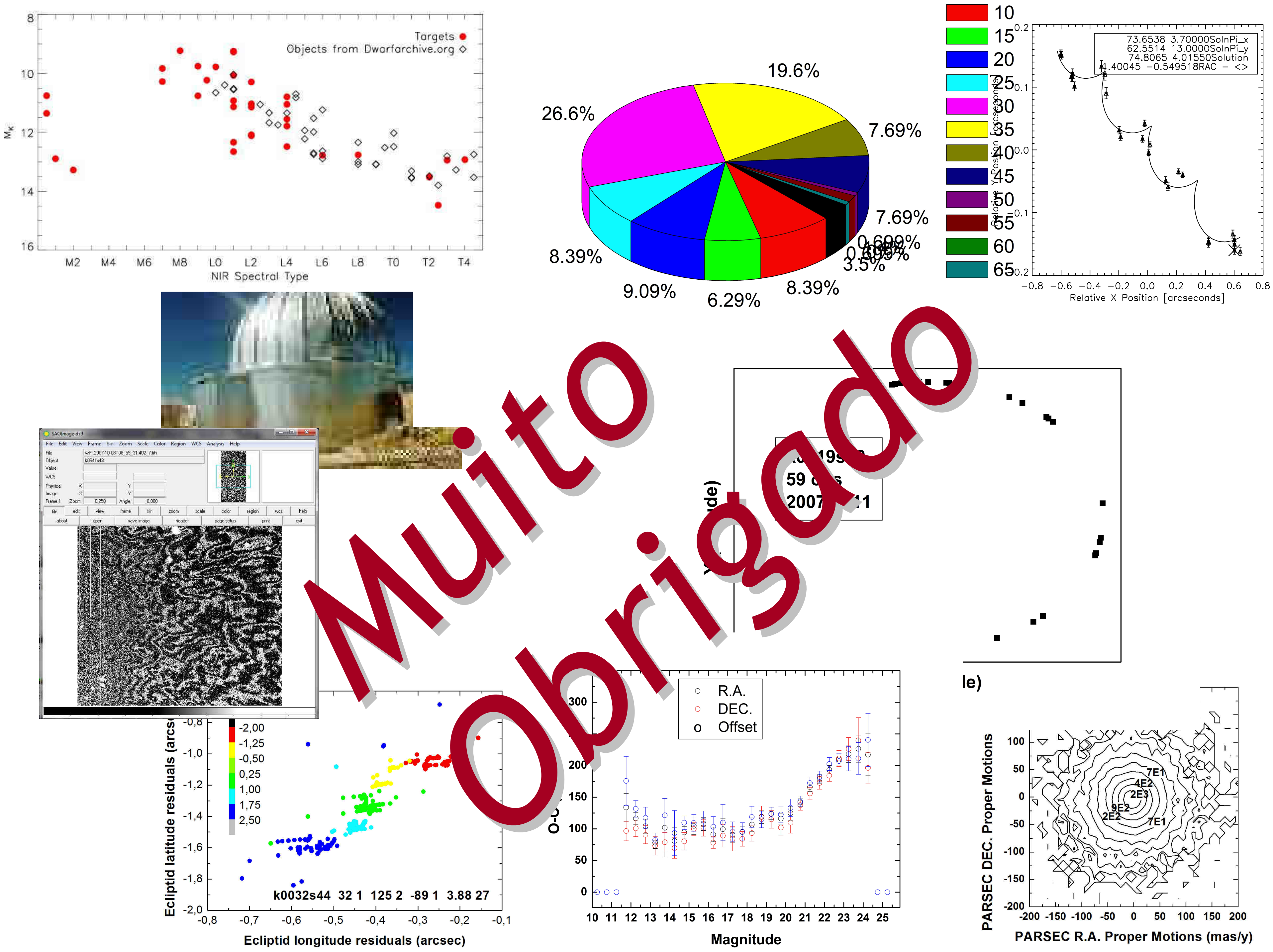

Muito
Obrigado
Targets
Objects from Dwarfarchive.org
NIR Spectral Type
19.6%
26.6%
7.69%
8.39%
9.09%
6.29%
Relative X Position [arcseconds]
R.A.
DEC.
Offset
Magnitude
Ecliptid latitude residuals (arcsec)
Ecliptid longitude residuals (arcsec)
k0032s44 32 1 125 2 -89 1 3.88 27
PARSEC DEC. Proper Motions
PARSEC R.A. Proper Motions (mas/y)